Pointing Error Engineering Tool

PointingSat Definition

Document Number:	ASTOS-PEET-TN-001		**Date:**
Issue:	1.2		2012-12-19

	Name/Function	**Organization**	**Signature**	
Prepared by:	M. Hirth	iFR		2012-12-19
	T. Ott	iFR		2012-12-19
	H. Su	iFR		2012-12-19
Checked by:	S. Weikert	Astos Solutions		2012-12-19
Product Assurance:	A. Wiegand	Astos Solutions		2012-12-19
Project Management:	S. Weikert	Astos Solutions		2012-12-19

Document Change Record

Issue	Date	Affected Chapter/Section/Page	Reason for Change Brief Description of Change
Draft 1	2012-04-02	All	Draft issue
Draft 2	2012-04-16	All	Update according to RIDs after PR1
1.0	2012-05-14	All	Update for working session
1.1	2012-11-29	All	Added references
1.2	2012-12-19	All	Updated according to final review

Table of Contents

1 Introduction

This document contains the definition of the PointingSat used within the PEET project. PointingSat describes an artificial precision pointing satellite mission with typical pointing error sources and system transfers. It serves as an example for a possible application of the methodology described in the ESA Pointing Error Engineering Handbook [AD1] concerning the setup and interpretation of pointing error sources and how to realize this methodology with the PEET software. Models and typical parameters are to a large extent based on inputs provided by ESA and [RD3]-[RD6].

This document has been prepared for the Project “Pointing Error Engineering Tool" (PEET) performed by Astos Solutions and Institute of Flight Mechanics and Control, University of Stuttgart as consultant under contract of the European Space Agency.

2 Applicable and Reference Documents

2.1 Applicable Documents

[AD1] ESSB-HB-E-003; ESA Pointing Error Engineering Handbook

[AD2] ECSS-E-ST-60-10C; Space Engineering, Control Performance

[AD3] ECSS-E-HB-60-10A; Space Engineering, Control Performance Guidelines

[AD4] IEEE-Std-952-1997 (R2008); IEEE Standard Specification Format Guide and Test Procedure for Single-Axis Interferometric Fiber Optic Gyros

2.2 Reference Documents

[RD1] Pittelkau M.E., Pointing Error Definitions, Metrics, and Algorithms, American Astronautical Society, AAS 03-559, p. 901, 2003.

[RD2] Graf, F.M., Covariance analysis and optimal estimator design, Student Research Project, 2011.

[RD3] Ott T., Benoit A., Van den Braembussche P., Fichter W., “ESA Pointing Error Engineering Handbook”, 8th International ESA Conference on Guidance, Navigation & Control Systems, Karlovy Vary CZ, June 2011.

[RD4] Ott T., Fichter W., Bennani S., Winkler S., "Precision Pointing H_∞ Control Design for Absolute, Window-, and Stability-Time Errors", accepted to be published in CEAS Space Journal.

[RD5] Hirth M., Brandt N., Fichter W., "Inertial Sensing for Future Gravity Missions", GEOTECHNOLOGIEN Science Report No.17, Observation of the System Earth from Space, Bonn, 2010, ISSN: 1619-7399.

[RD6] Hirth M., Fichter W., et al., "Optical Metrology Alignment and Impact on the Measurement Performance of the LISA Technology Package", Journal of Physics Conference Series, 7th International LISA Symposium, Barcelona, Spain, 2008.

3 Terms, Definitions and Abbreviated Terms

3.1 Acronyms

The following abbreviations are used throughout this document.

Acronyms	
AKE	Absolute Knowledge Error
APE	Absolute Performance Error
AST	Analysis Step
CRV	Time-Constant Random Variable
CTF	Coordinate Transformation
ESA	European Space Agency
FOV	Field Of View
KDE	Knowledge Drift Error
KRE	Knowledge Reproducibility Error
MKE	Mean Knowledge Error
MPE	Mean Performance Error
PDE	Performance Drift Error
PEC	Pointing Error Contributor
PEET	Pointing Error Engineering Tool
PES	Pointing Error Source
PRE	Performance Reproducibility Error
PSF	Point Spread Function
RP	Random Process
RPE	Relative Performance Error
RV	(Time-) Random Variable

3.2 Definitions

The following definitions are used in equations throughout this document.

Definitions	
α	Error on pointing level (rad)
B	Bias (representing a CRV)
BM(A)	Bimodal PDF with Amplitude A
δ()	Discrete distribution
$\varepsilon_D(D, \Delta t_D)$	Drift type PES with slope D and time span Δt_D
$G(\mu,\sigma^2)$	Gaussian PDF with mean μ and variance σ^2
n	Random process type PES in terms of PSD
P(f,A)	Periodic type PES with frequency f and amplitude A
T(t)	Time series
$U(e_{min}, e_{max})$	Uniform PDF between e_{min} and e_{max}

4 PointingSat Specification and Requirements

4.1 'Functional Requirements'

This section briefly summarizes general topics which shall be covered by the PointingSat example.

4.1.1 PES Representation

The set of PES for the PointingSat example shall cover at least one of the following representations:

- Time-constant random variables
- Periodic errors
- Random processes characterized by:
  - Time series
  - Covariance
  - Power spectral densities
- Time-random variables
- Drifts

4.1.2 Statistical Interpretation

The PointingSat example PES shall cover the following statistical interpretation types:

- Temporal interpretation
- Ensemble interpretation
- Mixed statistical interpretation

4.1.3 Pointing Error Index

The system pointing error requirements of PointingSat shall be characterized by:

- Dependency on instantaneous time only (e.g. AKE, APE)
- Dependency on a window time (e.g. MKE, MPE, RKE, RPE)
- Dependency on a stability time (e.g. KDE, KRE, PDE, PRE)

4.1.4 Correlation

The PointingSat example PES shall account for the following correlation states:

- Between axes of one PES (at least full or no correlation)
- Between different PES (at least full or no correlation)

4.1.5 System Transfer

The transfer from the PES of the PointingSat example to PEC shall at least be realized using the following system representations:

- Static system (e.g. coordinate transformation)
- Dynamic system (e.g. transfer functions)
- Feedback system
- Summation of PES

4.2 Mission and System Specification

PointingSat is a geostationary mission supporting the disaster assessment and monitoring for the European continent. The primary payload is a telescope for multi-spectral imaging (VIS, NIR, TIR, and MW) which allows detection and tracking of different ecological, economical and humanitarian incident follow-ups such as fires, algal bloom spread, oil slick or infrastructural damages after earthquakes, floods or windstorms.

As (dependent on the incident to be observed) the areas to be monitored are much larger than the payload FOV, highly accurate pointing and pointing stability of the satellite is required to allow single raster scanning of the relevant area on the one hand and repeated scanning of the same area in different spectral ranges.

Above mentioned image acquisition strategy and multi-channel usage leads to requirements on different kinds of pointing errors (error indices) whose general definitions are illustrated in the figure below.

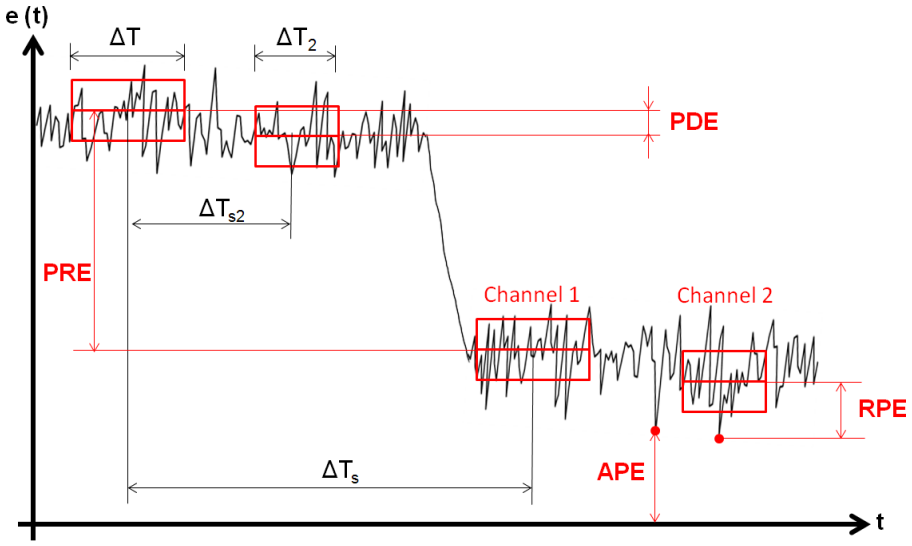

Figure 4-1: Different relevant error indices for PointingSat

As mentioned above, the main payload of PointingSat is a high-resolution telescope which is mounted on an ultra-stable optical bench. The IR focal planes are housed in cryostats and cooled by mechanical cryocoolers.

The PointingSat AOCS uses a star-tracker (2 camera heads in cold redundancy) and fibre-optical gyros (3+3 cold-redundant) for attitude and rate determination. A set of 10 cold-gas thrusters (thrust range from 1 μN to 0.5 mN) is used for the precision pointing attitude maneuvers.

4.3 Pointing Error Requirements

To achieve the mission objectives of PointingSat within the targeted accuracy, the following requirements on the system pointing error have to be met:

APE

The absolute steady-state pointing error during observations shall be smaller than 450 μrad (half-cone) with a level of confidence of P_c = 99.7% (n_p = 3).

$$\mathbf{e}_{APE} \leq \mathbf{e}_{APE,req} = 450\mu rad \approx 90\,arcsec \qquad \text{Eq 4-1}$$

As the mission objective is disaster monitoring, the main objective is to point during one entire observation period at the correct scene with a probability P_c. This requirement is driven by 'geo-location', i.e. images are acquired from the correct pointing scene of interest in order to reliably detect disasters.

This requires the application of the ensemble interpretation to ensure that the pointing error during one entire (100 % of time) observation k is less than $e_{APE,req}$.

RPE

The relative performance error within a time window ΔT = 0.5s shall be smaller than 10 μrad (half-cone) with a level of confidence of P_c = 68.2% (n_p = 1).

$$\mathbf{e}_{RPE} \leq \mathbf{e}_{RPE,req} = 10\mu rad \approx 2\,arcsec \qquad \text{Eq 4-2}$$

This requirement is driven by the need of a stable orientation throughout the integration time of the respective spectral channel (ΔT represents the maximum integration time out of the individual channels). The image quality is determined by the aberration of the point spread function during the integration time of a single observation. Pointing variations during exposure lead to a broadening of the point spread function and thus to aberration [RD1].

This error not only degrades the image quality, the raster/mosaic scan is affected as well. Pointing variations ε_{RPE} during exposure lead to a narrowing of the effective field of view as areas at the edge of the image are not covered at all time. Consequently the nominal image size h_{nom} is reduced to an effective image size h_{eff} and gaps between adjacent images may occur. This is illustrated in Figure 4-1 below. :

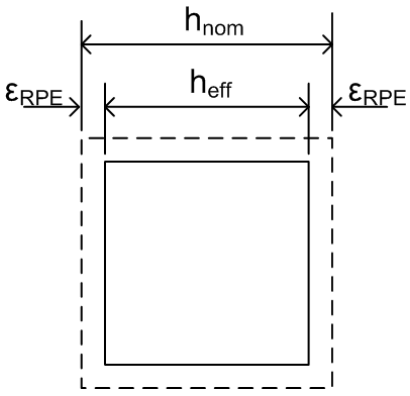

Figure 4-2: Impact of RPE on effective image size

As it has to be ensured that the RPE requirement is met for at least a fraction P_c of the overall integration time with 100% probability for sufficient image quality, temporal statistical interpretation applies in this case.

- **PRE (values TBC)**

The performance reproducibility error with respect to a window time of ΔT = 0.5s and a stability time ΔT_s = 600s shall be smaller than 50 μrad (half-cone) with a level of confidence of P_c = 99.7% (n_p = 3).

$$\mathbf{e}_{PRE} \leq \mathbf{e}_{PRE,req} = 50\mu rad \approx 10\,arcsec \qquad \text{Eq 4-3}$$

This requirement is driven by the need of a proper orientation between adjacent images of the scanning raster in case the target area cannot be covered by the telescope field of view. ΔT_s represents the total time required for one observation cycle, i.e. to achieve the full mosaic image. If a raster of N x M pictures is assumed (compare Figure 4-3), ΔT_s can be derived from:

$$\Delta T_s = N \cdot M \cdot \left(T_{slew} + T_{channels}\right) - T_{slew} \qquad \text{Eq 4-4}$$

where T_{slew} is the time required for the spacecraft reorientation to the next pointing scene and $T_{channels}$ represents the total time required for the image acquisition on all channels for one pointing scene[1].

The effect of the PRE can be illustrated as follows: Assume the nominal size of the field of view for one raster image is given by h_{nom} and a slew $d_{nom} = h_{nom}$ is commanded between each of the different pointing scenes. Then - dependent on its direction - a line of sight error motion of the first image (point spread function centroid) with respect to all other images (point spread function centroids) can result in gaps (black areas in Figure 4-3) or overlaps (dashed areas in Figure 4-3) between images.

In case of the PRE error mixed statistical interpretation applies as both the temporal and the ensemble behaviour are of interest.

[11] Note that generally another PDE requirement exists related to a stability time ΔT_{s2} (not treated here). This stability time corresponds to the adjustment/processing time between an acquisition of the same pointing scene on different channels. The respective window time ΔT_2 is then the same as the minimum window time ΔT of all channels.

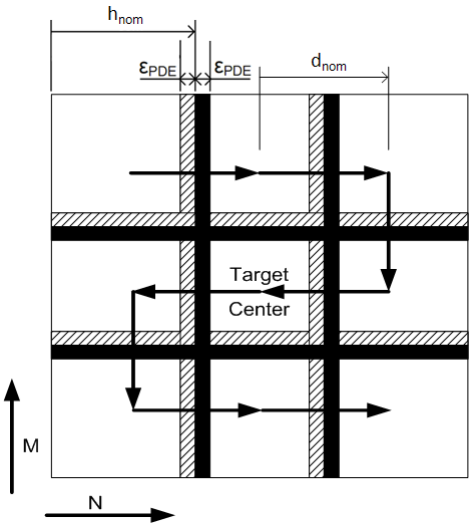

Figure 4-3: Impact of PRE on raster pointing sequence

4.4 Coordinate Frames

This section briefly describes the Cartesian coordinate frames used for the PES definitions and system transfers.

The origin of the **body reference frame** is located in the nominal center of mass of PointingSat. Its x-axis is aligned with the nominal line of sight direction of the payload telescope, the z-axis points in the direction of the solar panels and the y-axis completes the right-handed system (see Figure 4-4).

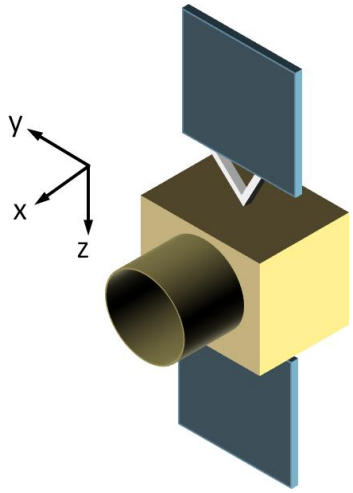

Figure 4-4: PointingSat body frame orientation

Assuming an ideal Nadir pointing direction of the satellite, the y-axis is then orientated ‘eastwards’ in the orbital plane and the z-axis points is perpendicular to the orbital plane (‘southwards’).

For the sake of simplicity of the PointingSat example the body frame is assumed to be identical to the **mechanical reference frame** of the satellite as well as to its **principal axis frame**.

The x-axis of the **payload reference frame** corresponds to the telescope boresight axis, its y- and z-axes represent the cross-boresight axes. Under nominal conditions, the payload axes are aligned with the axes of the body frame.

The **star tracker reference frame** defines the orientation of the axes of the sensor camera head. Its z-axis represents the boresight axis, x- and y-axes define the cross-boresight axes. The frame is linked to the body reference frame via a fixed coordinate-transformation (see section 5.4.2) depending on the sensor mounting direction.

5 Characterization of PES (AST-1)

The following subchapters describe in detail the definition of the PES which affect the pointing performance of PointingSat. This description includes information about modelling and the statistical interpretation.

Although not necessary from the requirements point of view, the statistical interpretation is presented for all different options in case of APE to highlight the influence of the interpretation.

The described PES can be roughly categorized as follows:

- Integration/Assembly errors: PES 1 and PES 2
- Actuator errors: PES 3
- Sensor errors:
  - Star tracker: PES 4 – PES 6
  - Gyro: PES 7
- Environmental errors: PES 8 – PES 13

5.1 PES 1: Mechanical Payload and Star Tracker Alignment

5.1.1 General Description

This PES represents the misalignment error knowledge between the payload axes and the star tracker axis expressed in the satellite body reference frame. Due to limitations of the manufacturing process itself, positioning of the payload telescope and the star tracker is only feasible within certain mechanical tolerances. Once assembled, a fixed misalignment error is present which is determined via theodolite measurements (and which can be compensated for in post-processing). However, the measuring device itself is also limited in its accuracy.

5.1.2 Model

As the PES is time-constant and the probability of measuring a certain misalignment value within the given tolerance of the measuring device is equal, it is modelled as zero mean CRV with uniform distribution, i.e.

$$\boldsymbol{\alpha}_1 = \begin{bmatrix} U(0,\alpha_{1,max,x}) \\ U(0,\alpha_{1,max,y}) \\ U(0,\alpha_{1,max,z}) \end{bmatrix} \text{arcsec} = \begin{bmatrix} U(0,30) \\ U(0,25) \\ U(0,27) \end{bmatrix} \text{arcsec} \qquad \text{Eq 5-1}$$

where $\alpha_{1,max,ax}$ describes the maximum knowledge error of the measurement process on axis `ax`).

5.1.3 Statistical Interpretation

The following statements about the statistical interpretation are in line with the descriptions given in Table B-3 of [AD3].

Note: Using PEET the user would only have to define a PES of CRV type, further interpretation is performed automatically for the user-selected statistical interpretation.

5.1.3.1 Temporal

RPE:

As the PES is time-constant it has no influence on the error, i.e.

$$\boldsymbol{\alpha}_{1,\text{temporal}} = \begin{bmatrix} 0 \\ 0 \\ 0 \end{bmatrix} \text{arcsec} \qquad \text{Eq 5-2}$$

APE (informative):

As the PES is time-constant, in case of a temporal interpretation the worst case 'bias' of the ensemble has to be taken into account, i.e.

$$\boldsymbol{\alpha}_{1,\text{temporal}} = \begin{bmatrix} \alpha_{1,\max,x} \\ \alpha_{1,\max,y} \\ \alpha_{1,\max,z} \end{bmatrix} \text{arcsec} \qquad \text{Eq 5-3}$$

5.1.3.2 Ensemble

APE:

In case of an ensemble interpretation, the PES can directly be described by the underlying PDF, i.e.

$$\boldsymbol{\alpha}_{1,\text{ensemble}} = \boldsymbol{\alpha}_1 \qquad \text{Eq 5-4}$$

5.1.3.3 Mixed

PRE:

Time-constant PES (which have in addition unchanged biases between observations) do not contribute to PRE errors, i.e.

$$\boldsymbol{\alpha}_{1,\text{mixed}} = \begin{bmatrix} 0 \\ 0 \\ 0 \end{bmatrix} \text{arcsec} \qquad \text{Eq 5-5}$$

APE (informative):

As there is no temporal distribution (time-constant PES), the mixed statistical interpretation simply reduces to the ensemble interpretation, i.e.

$$\boldsymbol{\alpha}_{1,\text{mixed}} = \boldsymbol{\alpha}_{1,\text{ensemble}} = \boldsymbol{\alpha}_{1} \qquad \text{Eq 5-6}$$

5.2 PES 2: Star Tracker to Payload Alignment after Launch

5.2.1 Description

This PES represents the alignment error between the star tracker axes and the payload axis resulting from the launch of the satellite. This misalignment arises first from distortions of the structure due to the transfer from 1g to 0g environment and second from permanent distortion induced by the vibration loads during the launch. However, once in orbit, this error remains constant over time.

5.2.2 Model

The PES is time-constant and numerous different structural elements might be subject to the distortions. According to this presetting, the PES can be modelled as zero mean CRV with Gaussian ensemble distribution, i.e.

$$\boldsymbol{\alpha}_{2} = \begin{bmatrix} G(0,\sigma_{2,x}^2) \\ G(0,\sigma_{2,y}^2) \\ G(0,\sigma_{2,z}^2) \end{bmatrix} \text{arcsec} = \begin{bmatrix} G(0,15^2) \\ G(0,10^2) \\ G(0,5^2) \end{bmatrix} \text{arcsec} \qquad \text{Eq 5-7}$$

where $\sigma_{2,ax}$ describes the standard deviation of the error on the respective axis `ax`.

5.2.3 Statistical Interpretation

The following statements about the statistical interpretation are in line with the descriptions given in Table B-3 of [AD3].

Note: Using PEET the user would only have to define a PES of CRV type, further interpretation is performed automatically for the user-selected statistical interpretation.

5.2.3.1 Temporal

- **RPE:**

As the PES is time-constant, it has no influence on the error, i.e.

$$\boldsymbol{\alpha}_{2,\text{temporal}} = \begin{bmatrix} 0 \\ 0 \\ 0 \end{bmatrix} \text{arcsec} \qquad \text{Eq 5-8}$$

- **APE (informative)**

As the PES is time-constant, in case of a temporal interpretation the worst case 'bias' of the ensemble has to be taken into account. The underlying Gaussian distribution is generally unbounded. However its worst case can be represented by the 3σ value, i.e.

$$\boldsymbol{\alpha}_{2,\text{temporal}} = \begin{bmatrix} 3\sigma_{2,x} \\ 3\sigma_{2,y} \\ 3\sigma_{2,z} \end{bmatrix} \text{arcsec} \qquad \text{Eq 5-9}$$

5.2.3.2 Ensemble

- **APE:**

In case of an ensemble interpretation, the PES can directly be described by the underlying PDF, i.e.

$$\boldsymbol{\alpha}_{2,\text{ensemble}} = \boldsymbol{\alpha}_2 \qquad \text{Eq 5-10}$$

5.2.3.3 Mixed

- **PRE:**

Time-constant PES (with additionally unchanged biases between observations) do not contribute to PRE errors, i.e.

$$\boldsymbol{\alpha}_{2,\text{mixed}} = \begin{bmatrix} 0 \\ 0 \\ 0 \end{bmatrix} \text{arcsec} \qquad \text{Eq 5-11}$$

- **APE (informative):**

As there is no temporal distribution (time-constant PES), the mixed statistical interpretation simply reduces to the ensemble interpretation, i.e. .

$$\boldsymbol{\alpha}_{2,\text{mixed}} = \boldsymbol{\alpha}_{2,\text{ensemble}} = \boldsymbol{\alpha}_2 \qquad \text{Eq 5-12}$$

5.3 PES 3: Thruster Noise

5.3.1 Description

This PES represents the actuation noise induced by one individual cold gas thruster. PointingSat uses clusters of identical thrusters of this type for attitude control.

The force noise acts along the thrust axis of the individual actuator frame. Assume that it has been characterized by the manufacturer in test facilities dependent on tank temperature and thrust level as follows:

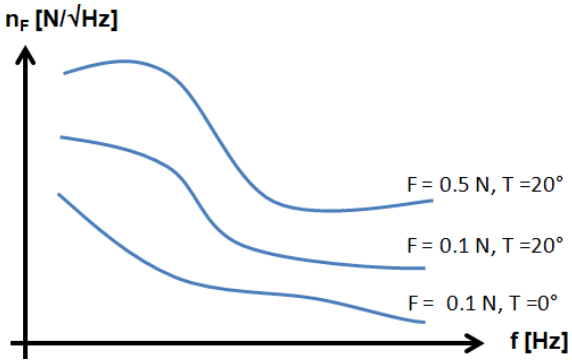

Figure 5-1: Thruster noise characteristics (exemplary)

5.3.2 Model

Assume that - given the characteristics from the datasheet - the PES can be modelled as, i.e.

$$\mathbf{n}_{F,3} = \mathrm{PSD}_3(f) \quad [\mathrm{N}/\sqrt{\mathrm{Hz}}] \qquad \text{Eq 5-13}$$

where PSD_3 describes the worst case spectrum of the force noise along the nominal thrust axis z. The worst case spectrum from the datasheet is chosen as sufficient information is not available for a proper description of the ensemble distribution (concerning temperature and thrust level). The PointingSat example thruster model is based on spectrum magnitude data imported from an Excel sheet (PES3_data.xls, sheet name 'freq_mag', range A1:B1000) and fitted to a transfer function of maximum order 14. The original data of PSD_3 together with the fitting result is shown below.

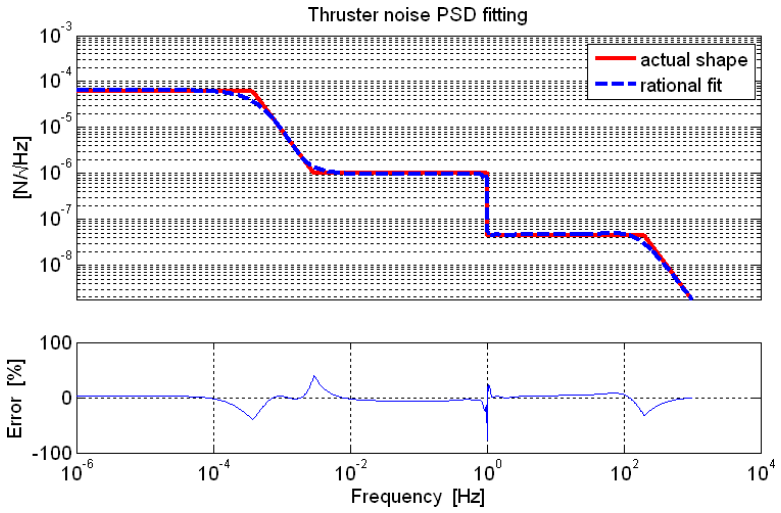

Figure 5-2: Thrust noise PSD

Above definition implies an ideal thrust realization in the desired direction and only 'one-dimensional' information is required. In case thruster misalignment errors (more precisely the knowledge of these errors) should be taken into account, generally two options exist:

- The noise power is defined by a one-dimensional spectrum for the thrust direction only. The misalignment and displacement of each thruster can individually be adapted by modifying the respective part in the actuation matrix (first block in Figure 6-3).

- The PES is already defined in terms of a resulting torque noise (after taking into account all individual displacements and misalignments in the actuation matrix that lead to a worst case torque noise on body axes) and the actuation matrix transfer in omitted.

All above options are supported by PEET, once the user has carried out the required calculations outside PEET. Indeed, the worst case of the torque noise on body axes depends on the design of the actuation concept (number, position and orientation of thrusters). The identification of this worst case is outside the scope of PEET.

5.3.3 Statistical Interpretation

The following statements about the statistical interpretation are in line with the descriptions given in Table 8-4 in [AD1].

Different to the case of RV or CRV type PES, the statistical interpretation is not applied at PES level (i.e. in advance of AST-2), but at PEC level after applying the metric filter for the error index to be evaluated. Interpretation at PEC level is necessary as any kind of system transfer affects the shape of the power spectrum as thus the related variance (this also justifies why the PES is described in terms of pointing error ($\boldsymbol{\alpha}$) and no longer on thrust level ($\mathbf{n}_F$) in the equations below).

Note: Using PEET the user would only have to define the PES of RP type, further interpretation is performed automatically for the user-selected statistical interpretation.

5.3.3.1 Temporal

- **RPE and APE:**

In case of a description in terms of PSD the PES can be described by the underlying Gaussian temporal distribution, i.e.

$$\boldsymbol{\alpha}_{3,\text{temporal}} = \begin{bmatrix} G(0,\sigma_{3,x}^2) \\ G(0,\sigma_{3,y}^2) \\ G(0,\sigma_{3,z}^2) \end{bmatrix} \text{rad} \qquad \text{Eq 5-14}$$

where $\sigma_{3,ax}$ is the standard deviation of the resulting PSD on pointing error level for axis `ax`.

5.3.3.2 Ensemble

- **APE:**

In case of a PES description in terms of PSD, the time-random behaviour of the underlying process is irrelevant. Thus, only the maximum noise value has to be taken into account which is represented by the 3σ-value of the Gaussian distribution, i.e.

$$\boldsymbol{\alpha}_{3,\text{ensemble}} = \begin{bmatrix} 3\sigma_{3,x} \\ 3\sigma_{3,y} \\ 3\sigma_{3,z} \end{bmatrix} \text{rad} \qquad \text{Eq 5-15}$$

where $\sigma_{3,ax}$ is the standard deviation of the resulting PSD on pointing error level for axis `ax`.

5.3.3.3 Mixed

- **PRE and APE:**

The mixed statistical interpretation corresponds to the temporal one, as the ensemble behaviour is constant, i.e.

$$\boldsymbol{\alpha}_{3,\text{mixed}} = \boldsymbol{\alpha}_{3,\text{temporal}} \qquad \text{Eq 5-16}$$

5.4 PES 4: Star Tracker Bias

5.4.1 Description

This PES represents the bias error knowledge of the star tracker measurement axes with respect to the nominal star tracker frame. It combines the contributions of on-ground calibration residuals and launch effects. Once in orbit, a fixed bias error is present.

5.4.2 Model

The PES is time-constant and the probability of obtaining a bias error within a given accuracy range of the calibration process is equal. The same is assumed for the launch effect contribution at this point. Thus, it is modelled as zero mean CRV with uniform distribution, i.e.

$$\boldsymbol{\alpha}_4 = \begin{bmatrix} U(0,\alpha_{4,\max,x}) \\ U(0,\alpha_{4,\max,y}) \\ U(0,\alpha_{4,\max,z}) \end{bmatrix} \text{arcsec} = \begin{bmatrix} U(0,8) \\ U(0,8) \\ U(0,7) \end{bmatrix} \text{arcsec} \qquad \text{Eq 5-17}$$

where $\alpha_{4,max,ax}$ describes the maximum error of the measurement process on axis `ax` and z represents the boresight axis of the star tracker.

5.4.3 Statistical Interpretation

The following statements about the statistical interpretation are in line with the descriptions given in Table B-3 of [AD3].

Note: Using PEET the user would only have to define a PES of CRV type, further interpretation is performed automatically for the user-selected statistical interpretation.

5.4.3.1 Temporal

- **RPE:**

As the PES is time-constant it has no influence on the error, i.e.

$$\boldsymbol{\alpha}_{4,\text{temporal}} = \begin{bmatrix} 0 \\ 0 \\ 0 \end{bmatrix} \text{arcsec} \qquad \text{Eq 5-18}$$

- **APE (informative):**

As the PES is time-constant, in case of a temporal interpretation the worst case 'bias' of the ensemble has to be taken into account, i.e.

$$\boldsymbol{\alpha}_{4,\text{temporal}} = \begin{bmatrix} \alpha_{4,\text{max},x} \\ \alpha_{4,\text{max},y} \\ \alpha_{4,\text{max},z} \end{bmatrix} \text{arcsec} \qquad \text{Eq 5-19}$$

5.4.3.2 Ensemble

- **APE:**

In case of an ensemble interpretation, the PES can directly be described by the underlying PDF, i.e.

5.4.3.3 Mixed

- **PRE:**

Time-constant PES (which have in addition unchanged biases between observations) do not contribute to PRE errors, i.e.

$$\boldsymbol{\alpha}_{4,\text{mixed}} = \begin{bmatrix} 0 \\ 0 \\ 0 \end{bmatrix} \text{arcsec} \qquad \text{Eq 5-20}$$

- **APE (informative):**

As there is no temporal distribution (time-constant PES), the mixed statistical interpretation simply reduces to the ensemble interpretation, i.e.

$$\boldsymbol{\alpha}_{4,\text{mixed}} = \boldsymbol{\alpha}_{4,\text{ensemble}} = \boldsymbol{\alpha}_{4} \qquad \text{Eq 5-21}$$

5.5 PES 5: Star Tracker Noise (Temporal)

5.5.1 Description

This PES represents the unprocessed attitude errors related to internal temporal noise of the star tracker unit such as read-out noise and quantization noise. This part of the noise is considered as independent of the operational conditions (e.g. temperature, star pattern in field of view). The error information for the different axes (around/across boresight) of this PES in the sensor frame is taken from the data sheet of the manufacturer. The data sheet provides the errors in the form of standard deviations of a random process for the across-boresight axes (x,y) and the around-boresight axis (z) together with a corresponding sampling time.

5.5.2 Model

With this information, the PES will be of RP type described by a covariance matrix, i.e. (displayed in vector form for compactness, as the non diagonal entries are zero):

$$\boldsymbol{\alpha}_5 = \begin{bmatrix} \sigma_{5,c}^2 \\ \sigma_{5,c}^2 \\ \sigma_{5,a}^2 \end{bmatrix} \text{arcsec}^2 = \begin{bmatrix} 1.2^2 \\ 1.2^2 \\ 8^2 \end{bmatrix} \text{arcsec}^2 \qquad \text{Eq 5-22}$$

where $\sigma_{5,c}$ describes the across-boresight standard deviation and $\sigma_{5,a}$ the standard deviation around boresight. The corresponding sampling time is 8Hz.

Note that in PEET this representation is converted to an equivalent PSD with white noise behaviour up to a cut-off frequency which corresponds to the Nyquist frequency of the given sampling time. Thus an equivalent expression of above PES is given by:

$$\boldsymbol{\alpha}_5 = \begin{bmatrix} PSD_{5,c} \\ PSD_{5,c} \\ PSD_{5,a} \end{bmatrix} \text{arcsec} / \sqrt{\text{Hz}} \qquad \text{Eq 5-23}$$

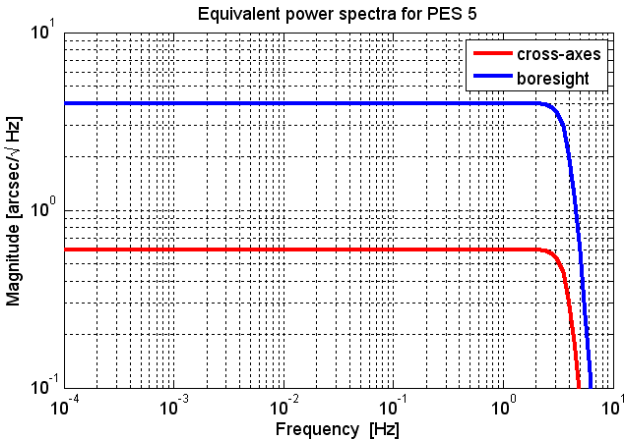

Figure 5-3: Equivalent temporal star tracker noise PSD

5.5.3 Statistical Interpretation

The following statements about the statistical interpretation are in line with the descriptions given in Table 8-4 in [AD1].

The statistical interpretation is applied at PEC level in case of RP type PES (see section 5.3.3), i.e. $\boldsymbol{\sigma}_{5,x}$, $\boldsymbol{\sigma}_{5,y}$ and $\boldsymbol{\sigma}_{5,z}$ are NOT equal to the initial $\boldsymbol{\sigma}_{5,c}$ in $\boldsymbol{\sigma}_{5,a}$!.

Note: Using PEET the user would only have to define the PES of RP type, further interpretation is performed automatically for the user-selected statistical interpretation.

5.5.3.1 Temporal

- **RPE and APE:**

In case of a description in terms of PSD the PES can be described by the underlying Gaussian distribution, i.e.

$$\boldsymbol{\alpha}_{5,\text{temporal}} = \begin{bmatrix} G(0,\sigma_{5,x}^2) \\ G(0,\sigma_{5,y}^2) \\ G(0,\sigma_{5,z}^2) \end{bmatrix} \text{rad} \qquad \text{Eq 5-24}$$

where $\sigma_{5,ax}$ is the standard deviation of the resulting PSD on pointing error level for axis `ax`.

5.5.3.2 Ensemble

- **APE:**

In case of a PES description in terms of PSD, the time-random behaviour of the underlying process is irrelevant. Thus, only the maximum noise value has to be taken into account which is represented by the 3σ-value of the Gaussian distribution, i.e.

$$\boldsymbol{\alpha}_{5,\text{ensemble}} = \begin{bmatrix} 3\sigma_{5,x} \\ 3\sigma_{5,y} \\ 3\sigma_{5,z} \end{bmatrix} \text{rad} \qquad \text{Eq 5-25}$$

where $\sigma_{5,ax}$ is the standard deviation of the resulting PSD on pointing error level for axis `ax`.

5.5.3.3 Mixed

- **PRE and APE:**

The mixed statistical interpretation corresponds to the temporal one, as the ensemble behaviour is constant, i.e.

$$\boldsymbol{\alpha}_{5,\text{mixed}} = \boldsymbol{\alpha}_{5,\text{temporal}} \qquad \text{Eq 5-26}$$

5.6 PES 6: Star Tracker FOV and Pixel Spatial Errors

5.6.1 Description

This PES represents the unprocessed attitude errors related to field of view and pixel noise of the star tracker unit. The error information for the different axes (around/across boresight) of this PES in the sensor frame is taken from the data sheet of the manufacturer. The data sheet provides the errors in the form of parameter values that define a power spectrum for both noise sources.

In general, both noise sources could be realized as single PES (or combined to an overall star tracker noise together with the temporal noise of PES 5). Additionally PEET offers a special block 'Star Tracker Noise' which allows a simple definition of the required parameters which are used to setup the model described below.

5.6.2 Model

- **FOV noise:**

The data sheet provides the following parameters for the FOV noise (for both cross-axes and boresight axis:

White noise level:	n_{FOV} = 0.8 arcsec
No. of tracked stars:	N_{stars} = 12
Detector size:	1024 Pixels

Note that the actual number of stars depends mainly on the tracking mode and the on the region of the sky that is being observed. Thus, N_{stars} should be considered as a typical average rather than being a fixed number. With the parameters above, the PSD of the FOV noise can be modelled using a 1st-order filter as:

$$PSD_{FOV} = \sqrt{\frac{T_{FOV}}{\left|1+s\frac{T_{FOV}}{2}\right|^2} n_{FOV}^2} \qquad [arcsec/\sqrt{Hz}] \qquad \text{Eq 5-27}$$

The correlation time T_{FOV} is assumed to be proportional to the inverse of the velocity v_{star} (pixels/sec) with which the star image moves on the sensor pixel matrix:

$$T_{FOV} = \frac{1024}{v_{star}\sqrt{N_{stars}}} \ [s] \qquad \text{Eq 5-28}$$

The star velocity itself can be linked to the spacecraft angular velocity ω_{SC} = 360°/day as follows:

$$v_{star} = \omega \frac{1024}{FOV} \sin\beta \cos\alpha \qquad \text{Eq 5-29}$$

where FOV is the sensor field of view in degrees, β is the angle between the sensor boresight and the spacecraft rotation axis and α is the angle between the star image direction of motion on the detector matrix and the reference axis.

The sensor field of view is assumed to be 30° and the sine-cosine product is set to 1 for the sake of simplicity.

The result is a correlation time of T_{FOV} = 2080s.

- **Pixel noise:**

The data sheet provides the following parameters for the pixel noise on the cross-axes (boresight axis):

White noise level:	n_{pixel} = 1.5 arcsec (12 arcsec)
Damping of 2nd order filter:	ξ = 0.6 (0.6)
Size of centroiding window:	N_{pixels} = 3 (3)
Detector size:	1024 Pixels

With these parameters, the PSD of the FOV noise can be modelled using a 2nd-order filter as:

$$PSD_{pixel} = \sqrt{\frac{\omega_0^4}{\left|s^2 + 2\xi\omega_0 s + \omega_0^2\right|^2} n_{pixel}^2 \, T_{pixel}} \quad [arcsec/\sqrt{Hz}] \qquad \text{Eq 5-30}$$

where the characteristic frequency ω_0 is given by:

$$\omega_0 = \frac{4\xi}{T_{pixel}} \qquad \text{Eq 5-31}$$

The correlation time T_{pixel} is again assumed to be proportional to the inverse of the velocity v_{star}:

$$T_{pixel} = \frac{N_{pixels}}{v_{star}} \; [s] \qquad \text{Eq 5-32}$$

with the star velocity computed as for the FOV noise case. The result is a correlation time of T_{pixel} = 21.1s.

The resulting power spectra for both noise sources are illustrated in the figure below:

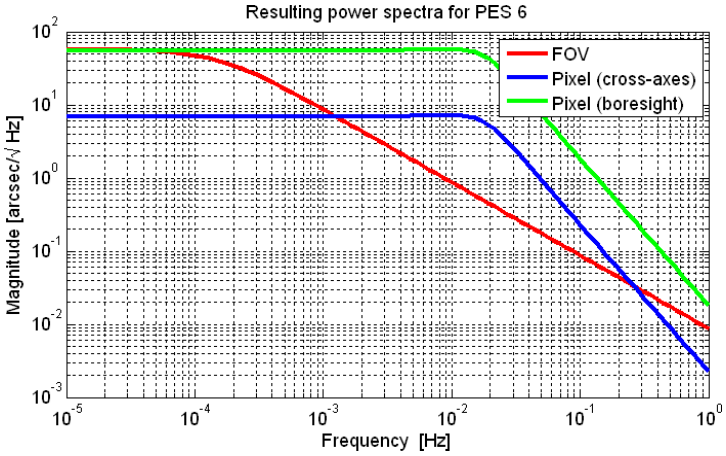

Figure 5-4: FOV and Pixel noise PSDs

- **Total noise:**

Assuming that FOV and pixel noise are uncorrelated, the total PSD for this PES is given by:

$$PSD_{6,ax} = \sqrt{PSD_{6,ax,pixel}^2 + PSD_{6,ax,FOV}^2}$$

Combining above results, PES 6 can be finally expressed as (see also Figure 5-5) :

$$\boldsymbol{\alpha}_6 = \begin{bmatrix} PSD_{6,c} \\ PSD_{6,c} \\ PSD_{6,a} \end{bmatrix} rad/\sqrt{Hz} \qquad \text{Eq 5-33}$$

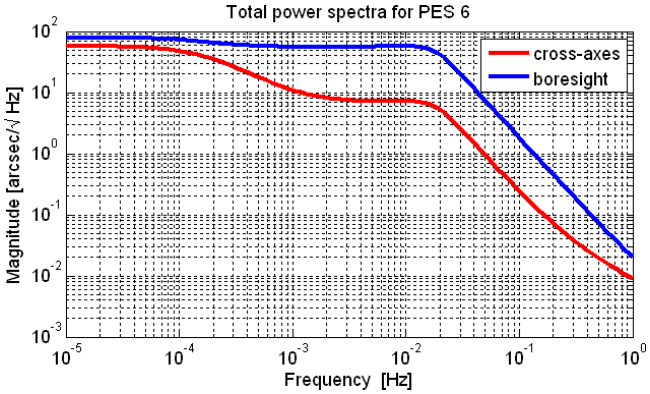

Figure 5-5: Total power spectra for PES 6

The following statements about the statistical interpretation are in line with the descriptions given in Table 8-4 in [AD1].

Note: Using PEET the user would only have to define the PES basic parameters, further interpretation is performed automatically for the user-selected statistical interpretation.

5.6.2.1 Temporal

- **RPE and APE:**

In case of a description in terms of PSD the PES can be described by the underlying Gaussian distribution, i.e.

$$\boldsymbol{\alpha}_{6,\text{temporal}} = \begin{bmatrix} G(0,\sigma_{6,x}^2) \\ G(0,\sigma_{6,y}^2) \\ G(0,\sigma_{6,z}^2) \end{bmatrix} \text{rad} \qquad \text{Eq 5-34}$$

where $\sigma_{6,ax}$ is the standard deviation of the resulting PSD on pointing error level for axis `ax`.

The statistical interpretation is applied at PEC level in this case (see section 5.3.3).

5.6.2.2 Ensemble

- **APE:**

In case of a PES description in terms of PSD, the time-random behaviour of the underlying process is irrelevant. Thus, only the maximum noise value has to be taken into account which is represented by the 3σ-value of the Gaussian distribution, i.e.

$$\boldsymbol{\alpha}_{6,\text{ensemble}} = \begin{bmatrix} 3\sigma_{6x} \\ 3\sigma_{6,y} \\ 3\sigma_{6,z} \end{bmatrix} \text{rad} \qquad \text{Eq 5-35}$$

where $\sigma_{6,ax}$ is the standard deviation of the resulting PSD on pointing error level for axis `ax`.

The statistical interpretation is applied at PEC level in this case (see section 5.3.3).

5.6.2.3 Mixed

- **PRE and APE:**

The mixed statistical interpretation corresponds to the temporal one, as the ensemble behaviour is constant, i.e.

$$\boldsymbol{\alpha}_{6,\text{mixed}} = \boldsymbol{\alpha}_{6,\text{temporal}} \qquad \text{Eq 5-36}$$

5.7 PES 7: Gyro Noise

5.7.1 Description

This PES represents the unprocessed noise on the rate measurements from a gyro assembly (one sensor aligned with each axis, thus the PES can be considered as already converted into the spacecraft body frame).

5.7.2 Model

Using typical specifications for a rate sensor, its noise characteristics can be described by:

Angle random walk:	N = 0.0005°/√h
Bias instability:	B = 0.001°/h
Rate random walk:	K = 0.0001°/h$^{3/2}$
Quantization noise:	Q = 3 arcsec
Sample period	T = 0.1s

According to Appendix B in [AD4], this description can be converted into a PSD representation as shown in the Figure below.

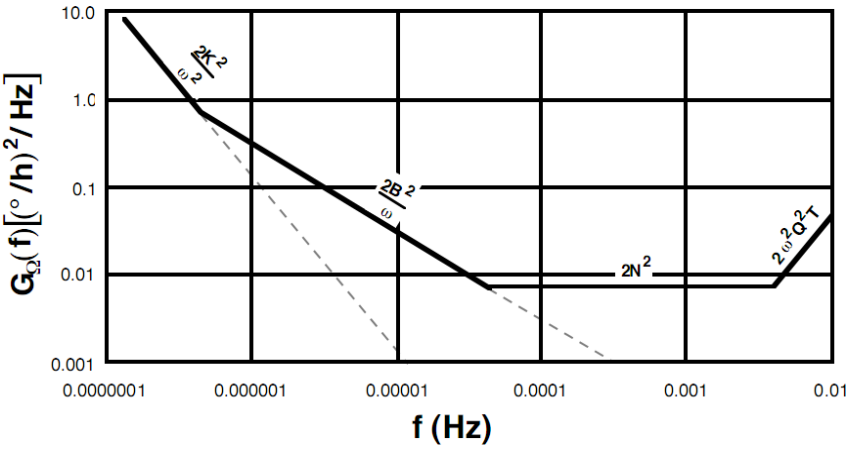

Figure 5-6: Gyro noise PSD derived from typical specifications [AD4] .

This PSD could either be defined manually by a set of frequency and magnitude vectors or simply using the special 'Gyro Rate Noise' block and providing the above-mentioned parameters. In both cases, PEET performs a rational fit (maximum order 16 in this example) of a transfer function magnitude to the above shape which can be represented by:

$$\mathbf{n}_{\omega,7} = \begin{bmatrix} PSD_{7,x} \\ PSD_{7,y} \\ PSD_{7,z} \end{bmatrix} rad/s \qquad \text{Eq 5-37}$$

where $PSD_{7,ax}$ describes the rate noise on the respective axis `ax` (identical in this case for all axes). For the parameters above, the resulting PSD is shown in Figure 5-7.

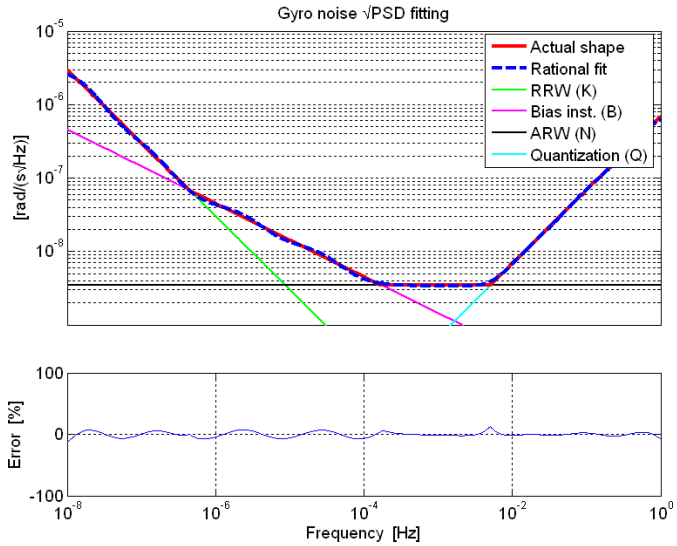

Figure 5-7: Gyro noise PSD for given parameters.

5.7.3 Statistical Interpretation

The following statements about the statistical interpretation are in line with the descriptions given in Table 8-4 in [AD1].

Note: Using PEET the user would only have to define the PES of RP type, further interpretation is performed automatically for the user-selected statistical interpretation.

5.7.3.1 Temporal

- **RPE and APE:**

In case of a description in terms of PSD the PES can be described by the underlying Gaussian distribution, i.e.

$$\boldsymbol{\alpha}_{7,\text{temporal}} = \begin{bmatrix} G(0,\sigma_{7,x}^2) \\ G(0,\sigma_{7,y}^2) \\ G(0,\sigma_{7,z}^2) \end{bmatrix} \text{rad} \qquad \text{Eq 5-38}$$

where $\sigma_{7,ax}$ is the standard deviation of the resulting PSD on pointing error level for axis `ax`.

The statistical interpretation is applied at PEC level in this case (see section 5.3.3).

5.7.3.2 Ensemble

- **APE:**

In case of a PES description in terms of PSD, the time-random behaviour of the underlying process is irrelevant. Thus, only the maximum noise value has to be taken into account which is represented by the 3σ-value of the Gaussian distribution, i.e.

$$\boldsymbol{\alpha}_{7,\text{ensemble}} = \begin{bmatrix} 3\sigma_{7,x} \\ 3\sigma_{7,y} \\ 3\sigma_{7,z} \end{bmatrix} \text{rad} \qquad \text{Eq 5-39}$$

where $\sigma_{7,ax}$ is the standard deviation of the resulting PSD on pointing error level for axis `ax`.

The statistical interpretation is applied at PEC level in this case (see section 5.3.3).

5.7.3.3 Mixed

- **PRE and APE:**

The mixed statistical interpretation corresponds to the temporal one, as the ensemble behaviour is constant, i.e.

$$\boldsymbol{\alpha}_{7,\text{mixed}} = \boldsymbol{\alpha}_{7,\text{temporal}} \qquad \text{Eq 5-40}$$

5.8 PES 8: Environmental Disturbances

5.8.1 Description

This PES represents noise induced by external environmental disturbance torques. In case of PointingSat, the solar radiation pressure is identified as the driving disturbance source with minor influence of the gravity gradient and magnetic field torques only.

5.8.2 Model

Simulations using worst case model settings for the satellite environment and a simplified satellite surface model have been performed for PointingSat. The matching set of results is represented by:

$$\mathbf{T}_8 = \begin{bmatrix} T_x(t) \\ T_y(t) \\ T_z(t) \end{bmatrix} \text{Nm} \qquad \text{Eq 5-41}$$

where $T_{8,ax}$ describes the disturbance torque time series for the respective axis `ax` (shown in Figure 5-8).

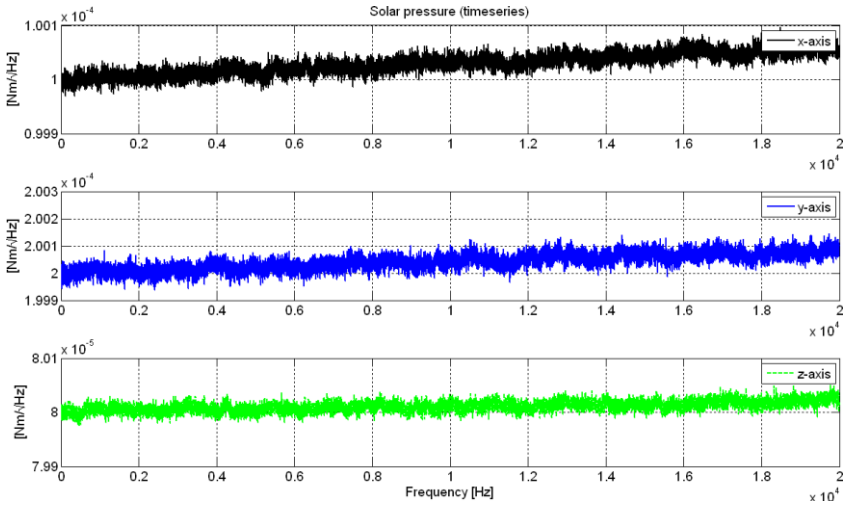

Figure 5-8: Time series of environmental disturbance noise

The data is imported from Excel (PES8_data.xls,sheet name 'solarpressure_time_series', range A1:D20000) and represents a time series of 20000s at 1Hz sampling. PEET automatically computes the PSD (auto- and cross-spectra) from the time series and fits the result to a transfer function with equivalent magnitude (maximum pole order 5 for this example).

The time series include torque biases as well as the noise and drift properties of the disturbances, thus implicitly different PES types are covered:

- **Bias:**

The bias derived from each axes time series is a time constant discrete which is covered by a CRV type PES. Formally it is represented by a discrete distribution, i.e.

$$\mathbf{B}_8 = \begin{bmatrix} \delta(B_{9,x}) \\ \delta(B_{9,y}) \\ \delta(B_{9,z}) \end{bmatrix} \mathrm{Nm} = \begin{bmatrix} 1.0 \\ 2.0 \\ 0.8 \end{bmatrix} \mathrm{mNm} \qquad \text{Eq 5-42}$$

where $B_{9,ax}$ describes the respective bias value on axis `ax`.

- **Drift:**

The linear trend in the time series is modelled as a drift type PES using the slope D of the trend and the overall time span of the time series, i.e.

$$\boldsymbol{\varepsilon}_{D,8} = \begin{bmatrix} \varepsilon_D(D_{8,x}, \Delta t_{8,D}) \\ \varepsilon_D(D_{8,y}, \Delta t_{8,D}) \\ \varepsilon_D(D_{8,z}, \Delta t_{8,D}) \end{bmatrix} \mathrm{Nm/s} = \begin{bmatrix} \varepsilon_D(3 \cdot 10^{-12}, 10^6 \mathrm{s}) \\ \varepsilon_D(4 \cdot 10^{-12}, 10^6 \mathrm{s}) \\ \varepsilon_D(1 \cdot 10^{-12}, 10^6 \mathrm{s}) \end{bmatrix} \mathrm{Nm/s} \qquad \text{Eq 5-43}$$

where $D_{8,ax}$ describes the respective drift rate for axis `ax` and $\Delta t_{8,D}$ the overall time span of the time series.

Note that $\Delta t_{8,D}$ should be much larger than the window time and stability time for the RPE and PRE indices to properly describe the drift.

As the drift is derived from one single set of time series, the drift rate $D_{8,ax}$ is a discrete value. Formally it is interpreted as a worst case value $D_{8,WC,ax}$.

- **Noise:**

The remaining part after bias removal and detrending is described as an RP type PES in terms of PSD, i.e.

$$\mathbf{n}_{Trq,8} = \begin{bmatrix} PSD_{8,xx} \\ PSD_{8,yy} \\ PSD_{8,zz} \end{bmatrix} Nm/\sqrt{Hz} \qquad \text{Eq 5-44}$$

where $PSD_{8,ax\text{-}ax}$ describes the noise auto power spectral density on axis `ax`.

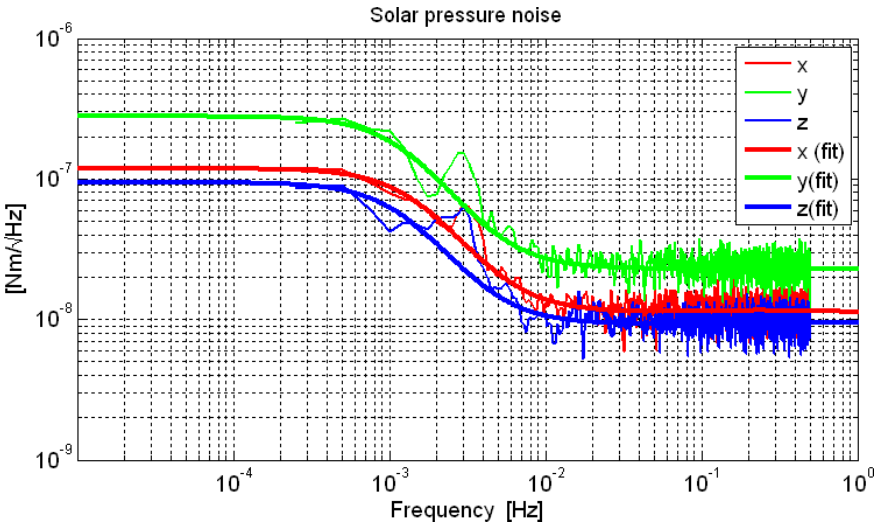

Figure 5-9: Solar pressure torque noise (PSD and fit).

Note that above-mentioned subdivision into 3 PES types is automatically performed using PEET.

5.8.3 Statistical Interpretation

The following statements about the statistical interpretation are in line with the descriptions given in Table B-3 of [AD3] (CRV), Table B-7 of [AD3] (Drift) and Table 8-4 of [AD1] (RP).

5.8.3.1 Temporal

- **Bias:**

RPE:

As the PES is time-constant, it has no influence on the error, i.e.

$$\mathbf{B}_{8,\text{temporal}} = \begin{bmatrix} 0 \\ 0 \\ 0 \end{bmatrix} \text{Nm} \qquad \text{Eq 5-45}$$

APE (informative):

As the PES is time-constant, in case of a temporal interpretation the worst case bias of the ensemble would have to be taken into account. As it has a discrete distribution, this is simply the determined bias, i.e.

$$\mathbf{B}_{8,\text{temporal}} = \begin{bmatrix} B_{8,\text{max},x} \\ B_{8,\text{max},y} \\ B_{8,\text{max},z} \end{bmatrix} \text{Nm} = \begin{bmatrix} B_{8,x} \\ B_{8,y} \\ B_{8,z} \end{bmatrix} \text{Nm} \qquad \text{Eq 5-46}$$

- **Drift:**

RPE:

With above mentioned formal definitions, the PES can be described by:

$$\boldsymbol{\varepsilon}_{D,8,\text{temporal}} = \begin{bmatrix} U(-\frac{\Delta T}{2} D_{8,WC,x}, \frac{\Delta T}{2} D_{8,WC,x}) \\ U(-\frac{\Delta T}{2} D_{8,WC,y}, \frac{\Delta T}{2} D_{8,WC,y}) \\ U(-\frac{\Delta T}{2} D_{8,WC,z}, \frac{\Delta T}{2} D_{8,WC,z}) \end{bmatrix} \text{Nm} = \begin{bmatrix} U(-\frac{\Delta T}{2} D_{8,x}, \frac{\Delta T}{2} D_{8,x}) \\ U(-\frac{\Delta T}{2} D_{8,y}, \frac{\Delta T}{2} D_{8,y}) \\ U(-\frac{\Delta T}{2} D_{8,z}, \frac{\Delta T}{2} D_{8,z}) \end{bmatrix} \text{Nm} \qquad \text{Eq 5-47}$$

where ΔT is the window time from the RPE requirement (see chapter 4.3).

APE (informative):

With above mentioned formal definitions, the PES can be described by:

$$\boldsymbol{\varepsilon}_{D,8,\text{temporal}} = \begin{bmatrix} U(0, \Delta t_{8,D} D_{8,WC,x}) \\ U(0, \Delta t_{8,D} D_{8,WC,y}) \\ U(0, \Delta t_{8,D} D_{8,WC,z}) \end{bmatrix} \text{Nm} = \begin{bmatrix} U(0, \Delta t_{8,D} D_{8,x}) \\ U(0, \Delta t_{8,D} D_{8,y}) \\ U(0, \Delta t_{8,D} D_{8,z}) \end{bmatrix} \text{Nm} \qquad \text{Eq 5-48}$$

- **Noise:**

RPE and APE:

In case of a description in terms of PSD the PES can be described by the underlying Gaussian distribution, i.e.

$$\boldsymbol{\alpha}_{8,\text{temporal}} = \begin{bmatrix} G(0, \sigma^2_{8,x}) \\ G(0, \sigma^2_{8,y}) \\ G(0, \sigma^2_{8,z}) \end{bmatrix} \text{rad} \qquad \text{Eq 5-49}$$

where $\sigma_{8,ax}$ is the standard deviation of the resulting PSD on pointing error level for axis `ax`.

The statistical interpretation is applied at PEC level in this case (see section 5.3.3).

5.8.3.2 Ensemble

- **Bias:**

APE:

In case of an ensemble interpretation, the PES can directly be described by the underlying PDF, i.e.

$$\mathbf{B}_{8,ensemble} = \mathbf{B}_8 = \begin{bmatrix} \delta(B_{8,x}) \\ \delta(B_{8,y}) \\ \delta(B_{8,z}) \end{bmatrix} Nm = \begin{bmatrix} B_{8,x} \\ B_{8,y} \\ B_{8,z} \end{bmatrix} Nm \qquad \text{Eq 5-50}$$

- **Drift:**

APE:

With above mentioned formal definitions, the PES can be described by:

$$\boldsymbol{\varepsilon}_{8,ensemble} = \frac{1}{\Delta t_{8,D}} = \begin{bmatrix} \delta(D_{8,x}) \\ \delta(D_{8,y}) \\ \delta(D_{8,z}) \end{bmatrix} Nm \qquad \text{Eq 5-51}$$

- **Noise:**

APE:

In case of a PES description in terms of PSD, the time-random behaviour of the underlying process is irrelevant. Thus, only the maximum noise value has to be taken into account which is represented by the 3σ-value of the Gaussian distribution, i.e.

$$\boldsymbol{\alpha}_{8,ensemble} = \begin{bmatrix} 3\sigma_{8,x} \\ 3\sigma_{8,y} \\ 3\sigma_{8,z} \end{bmatrix} rad \qquad \text{Eq 5-52}$$

where $\sigma_{8,ax}$ is the standard deviation of the resulting PSD on pointing error level for axis `ax`.

The statistical interpretation is applied at PEC level in this case (see section 5.3.3).

5.8.3.3 Mixed

- **Bias:**

PRE:

Time-constant PES (with unchanged biases between observations) do not contribute to PRE errors, i.e.

$$\mathbf{B}_{8,mixed} = \begin{bmatrix} 0 \\ 0 \\ 0 \end{bmatrix} Nm \qquad \text{Eq 5-53}$$

APE (informative):

As there is no temporal distribution (time-constant PES), the mixed statistical interpretation simply reduces to the ensemble interpretation, i.e.

$$\mathbf{B}_{8,mixed} = \mathbf{B}_{8,ensemble} = \mathbf{B}_8 \qquad \text{Eq 5-54}$$

- **Drift:**

PRE:

Drift type PES do not contribute to PRE by definition, thus:

$$\boldsymbol{\varepsilon}_{D,8,mixed} = \begin{bmatrix} 0 \\ 0 \\ 0 \end{bmatrix} Nm \qquad \text{Eq 5-55}$$

PDE (informative):

Different to the PRE, the PES would contribute to a PDE as follows:

$$\boldsymbol{\varepsilon}_{D,8,mixed} = \frac{1}{\Delta T_{s2}} \begin{bmatrix} \delta(D_{8,x}) \\ \delta(D_{8,y}) \\ \delta(D_{8,z}) \end{bmatrix} Nm \qquad \text{Eq 5-56}$$

where ΔT_{s2} is the stability time from the (omitted) PDE requirement (see footnote in chapter 4.3).

APE (informative):

Following Table B-7 in [AD3], the PES can be described by:

$$\boldsymbol{\varepsilon}_{D,8,mixed} = \begin{bmatrix} \int PDF(\varepsilon_{D,8,x} \mid D_{8,x}) PDF(D_{8,x})\, dD_{8,x} \\ \int PDF(\varepsilon_{D,8,y} \mid D_{8,y}) PDF(D_{8,y})\, dD_{8,y} \\ \int PDF(\varepsilon_{D,8,z} \mid D_{8,z}) PDF(D_{8,z})\, dD_{8,z} \end{bmatrix} Nm \qquad \text{Eq 5-57}$$

where $\varepsilon_{D,8} = D_8 \cdot t$ describes the drift error (axis index omitted). As this relation is linear between zero and Δt_8, the conditional probability can be described by a uniform distribution. As the drift rate distribution is already known, the relevant statistical properties for $\varepsilon_{8,mixed}$ can be computed according to Appendix B.7 of [AD2] or directly derived from Table B-7 in [AD3].

- **Noise:**

PRE and APE:

The mixed statistical interpretation corresponds to the temporal one, as the ensemble behaviour is constant, i.e.

$$\boldsymbol{\alpha}_{8,\text{mixed}} = \boldsymbol{\alpha}_{8,\text{temporal}} \qquad \text{Eq 5-58}$$

5.9 PES 9: Thermo-Elastic Distortion (Periodic Part)

5.9.1 Description

This PES represents periodic part at orbital frequency (1/day) of thermo-elastic distortion between the payload and star tracker axes. The amplitude of this periodic error is assumed to be dependent on the DC operational temperature.

5.9.2 Model

As the PES describes a periodic signal, it can be modelled as PES of RP type Periodic. This type is defined by its frequency and the distribution of the amplitude. Assuming a linear dependence on the DC temperature which is required to be within a defined operation range only, the amplitude of the PES can be modelled with a uniform distribution, i.e.

$$\boldsymbol{\alpha}_9 = \begin{bmatrix} P(f_9, U(A_{9,\min,x}, A_{10,\max,x})) \\ P(f_9, U(A_{9,\min,y}, A_{10,\max,y})) \\ P(f_9, U(A_{9,\min,z}, A_{10,\max,z})) \end{bmatrix} = \begin{bmatrix} P(f_9, U(5,15) \\ P(f_9, U(4,10) \\ P(f_9, U(1,5) \end{bmatrix} \text{arcsec} \qquad \text{Eq 5-59}$$

where $A_{9,\min,ax}$ ($A_{9,\max,ax}$) describes the distortion amplitude for the respective axis ax (related to the minimum (maximum) permitted operational DC temperature) and f_9 = 1/day the frequency of the signal.

5.9.3 Statistical Interpretation

The following statements about the statistical interpretation are in line with the descriptions given in Table 8-5 in [AD1].

Generally the statistical interpretation is not applied at PES level for RP type PES but at PEC level (see section 5.3.3), i.e. the $A_{9,i}$ in the following subsections would have to replaced by resulting $A'_{9,i}$ after system transfer (in case any system transfer would be present in AST-2).

Note: Using PEET the user would only have to define the PES of RP type Periodic, further interpretation is performed automatically for the user-selected statistical interpretation.

5.9.3.1 Temporal

- **RPE and APE:**

In case of a description in terms of RP type Periodic, the PES can be described by a bimodal distribution characterized by the worst case amplitude, i.e.

$$\boldsymbol{\alpha}_{9,\text{temporal}} = \begin{bmatrix} \text{BM}(A_{9,\max,x}) \\ \text{BM}(A_{9,\max,y}) \\ \text{BM}(A_{9,\max,z}) \end{bmatrix} \text{rad} \qquad \text{Eq 5-60}$$

5.9.3.2 Ensemble

- **APE:**

In case of a description in terms of RP type Periodic, the PES can simply be described by a by the amplitude distribution, i.e.

$$\boldsymbol{\alpha}_{9,\text{ensemble}} = \begin{bmatrix} U(A_{9,\min,x}, A_{9,\max,x}) \\ U(A_{9,\min,y}, A_{9,\max,y}) \\ U(A_{9,\min,z}, A_{9,\max,z}) \end{bmatrix} \text{rad} \qquad \text{Eq 5-61}$$

5.9.3.3 Mixed

- **PRE and APE:**

In case of a mixed statistical interpretation again conditional probability has to be taken into account, i.e.

$$\boldsymbol{\alpha}_{9,\text{mixed}} = \begin{bmatrix} \int \text{BM}(A_{9,x})\, U(A_{9,\min,x}, A_{9,\max,x})\, dA_{9,x} \\ \int \text{BM}(A_{9,y})\, U(A_{9,\min,y}, A_{9,\max,y})\, dA_{9,y} \\ \int \text{BM}(A_{9,z})\, U(A_{9,\min,z}, A_{9,\max,z})\, dA_{9,z} \end{bmatrix} \text{Nm} \qquad \text{Eq 5-62}$$

where $A_{9,ax}$ represent the time-random variable/PES magnitude. The statistical properties for this case can be calculated according to Appendix B.7 of [AD2].

5.10 PES 10: Thermo-Elastic Distortion (Random Part)

5.10.1 Description

This PES represents the random/noise part of the thermo-elastic distortion between the payload and star tracker axes. There is no exact model available for this effect, only a linear dependence on the operational DC temperature is expected.

5.10.2 Model

According to these presetting, the random part can be modelled as a RV type PES with zero mean and Gaussian distribution. The variance of the PES is not constant, but uniformly distributed between upper and lower bounds related to effective DC operational temperature.

$$\boldsymbol{\alpha}_{10} = \begin{bmatrix} G(0, U(\sigma^2_{10,min,x}, \sigma^2_{10,max,x})) \\ G(0, U(\sigma^2_{10,min,y}, \sigma^2_{10,max,y})) \\ G(0, U(\sigma^2_{10,min,z}, \sigma^2_{10,max,z})) \end{bmatrix} \text{arcsec} = \begin{bmatrix} G(0, U(1,4)) \\ G(0, U(1,4)) \\ G(0, U(1,4)) \end{bmatrix} \text{arcsec} \quad \text{Eq 5-63}$$

where $\sigma_{10,min,ax}$ and $\sigma_{10,max,ax}$ describe the standard deviation on the axis `ax` related to the minimum and maximum DC operational temperature range.

5.10.3 Statistical Interpretation

The following statements about the statistical interpretation are in line with the descriptions given in Table B-2 in [AD3] and Table B-5 in [AD1].

5.10.3.1 Temporal

- **RPE and APE:**

In case of a description in terms of RV type, the PES can be described using the worst case variance of the underlying ensemble distribution the worst case amplitude, i.e.

$$\boldsymbol{\alpha}_{10,temporal} = \begin{bmatrix} G(0, \sigma^2_{10,max,x}) \\ G(0, \sigma^2_{10,max,y}) \\ G(0, \sigma^2_{10,max,z}) \end{bmatrix} \text{rad} \quad \text{Eq 5-64}$$

5.10.3.2 Ensemble

- **APE:**

In case of ensemble interpretation, the time-random behaviour of the RV type PES is irrelevant and only the ensemble distribution is of interest, i.e.

$$\boldsymbol{\alpha}_{11,ensemble} = \frac{1}{3} \begin{bmatrix} U(\sigma^2_{10,min,x}, \sigma^2_{10,max,x}) \\ U(\sigma^2_{10,min,y}, \sigma^2_{10,max,y}) \\ U(\sigma^2_{10,min,z}, \sigma^2_{10,max,z}) \end{bmatrix} \text{rad} \quad \text{Eq 5-65}$$

The factor 1/3 accounts for the fact that the Gaussian distribution is unbounded and a bound and 3σ level is imposed.

5.10.3.3 Mixed

- **PRE:**

PES of RV type with Gaussian temporal distribution have no contribution to PRE errors, i.e.

$$\boldsymbol{\alpha}_{10,mixed} = \begin{bmatrix} 0 \\ 0 \\ 0 \end{bmatrix} \text{rad} \quad \text{Eq 5-66}$$

- **APE (informative):**

In case of a mixed statistical interpretation again conditional probability has to be taken into account, i.e.

$$\boldsymbol{\alpha}_{10,\text{mixed}} = \begin{bmatrix} \int G(0,\sigma^2_{10,,x})\, U(\sigma^2_{10,\min,x},\sigma^2_{10,\max,x})\ d\sigma_{10,x} \\ \int G(0,\sigma^2_{10,,y})\, U(\sigma^2_{10,\min,y},\sigma^2_{10,\max,y})\ d\sigma_{10,y} \\ \int G(0,\sigma^2_{10,,z})\, U(\sigma^2_{10,\min,z},\sigma^2_{10,\max,z})\ d\sigma_{10,z} \end{bmatrix} \text{rad} \qquad \text{Eq 5-67}$$

The statistical properties for this case can be calculated according to Appendix B.7 of [AD2] or directly obtained from Tables B-2 and B-9 of [AD3].

5.11 PES 11: Thermal Stability Effect on Star Tracker

5.11.1 Description

This PES represents a temperature dependent part of the noise in the star tracker measurement, e.g. thermal distortions of the detector pixel array. From analysis, only the temperature stability at one reference point on the optical bench is known and the transfer behaviour from this reference to star tracker detector has been estimated.

5.11.2 Model

The temperature stability at the reference point is given in terms of a power spectrum leading to a PES model of the form:

$$\mathbf{n}_{T,11} = \text{PSD}_{11} \quad [\text{K}/\sqrt{\text{Hz}}] \qquad \text{Eq 5-68}$$

Note that the described temperature stability is 'one-dimensional', i.e. it cannot be assigned to a physical pointing axis at this point. Proper mapping to physical axis is then realized in the system transfer models. The model used to describe the temperature stability at the measured reference points is given by the following equation (illustrated in Figure 5-10)

$$\text{PSD}_{11} = 0.5 \cdot \frac{f_{T0}}{f} \quad [\text{K}/\sqrt{\text{Hz}}] \qquad \text{Eq 5-69}$$

with f_{T0} = 0.1 mHz.

To highlight the different options for PES definition in PEET, PES 11 is set up as a state-space model equivalent to the transfer function given above:

$$A = 0 \qquad B = 0.01563 \qquad C = 0.02011 \qquad D = 0 \qquad \text{Eq 5-70}$$

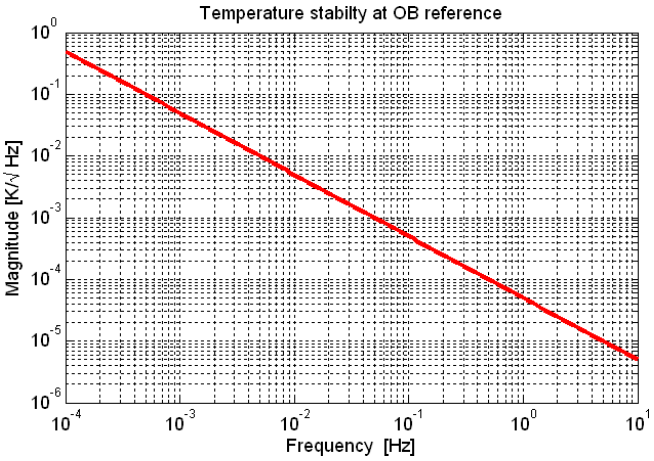

Figure 5-10: Thermal stability at optical bench reference point

5.11.3 Statistical Interpretation

The following statements about the statistical interpretation are in line with the descriptions given in Table 8-4 in [AD1].

The statistical interpretation is applied at PEC level in case of RP type PES (see section 5.3.3).

5.11.3.1 Temporal:

- **RPE and APE:**

Being defined in terms of PSD the PES can be described by the underlying Gaussian distribution, i.e.

$$\boldsymbol{\alpha}_{11,\text{temporal}} = \begin{bmatrix} G(0,\sigma^2_{11,x}) \\ G(0,\sigma^2_{11,y}) \\ G(0,\sigma^2_{11,z}) \end{bmatrix} \text{rad} \qquad \text{Eq 5-71}$$

where $\sigma_{11,ax}$ is the standard deviation of the resulting PSD on pointing error level for axis `ax`.

5.11.3.2 Ensemble

- **APE:**

In case of a PES description in terms of PSD, the time-random behaviour of the underlying process is irrelevant. Thus, only the maximum noise value has to be taken into account which is represented by the 3σ-value of the Gaussian distribution, i.e.

$$\boldsymbol{\alpha}_{11,\text{ensemble}} = \begin{bmatrix} 3\sigma_{11,x} \\ 3\sigma_{11,y} \\ 3\sigma_{11,z} \end{bmatrix} \text{rad} \qquad \text{Eq 5-72}$$

where $\sigma_{11,ax}$ is the standard deviation of the resulting PSD on pointing error level for axis `ax`.

5.11.3.3 Mixed

- **PRE and APE:**

The mixed statistical interpretation corresponds to the temporal one, as the ensemble behaviour is constant, i.e.

$$\boldsymbol{\alpha}_{11,\text{mixed}} = \boldsymbol{\alpha}_{11,\text{temporal}} \qquad \text{Eq 5-73}$$

5.12 PES 12: Thermal Stability Effect on Payload

5.12.1 Description

This PES represents a temperature stability induced noise that affects the position of the focal point of the telescope and in consequence directly the pointing. From analysis - as in case of PES 11 - only the temperature stability at one reference point on the optical bench is known and the transfer behaviour to from this reference to the focal point location has been estimated.

5.12.2 Model

The temperature stability at the reference point is given in terms of a power spectrum leading to a PES model of the form:

$$n_{T,12} = n_{T,11} = \text{PSD}_{11}\ \text{K}/\sqrt{\text{Hz}} \qquad \text{Eq 5-74}$$

Again, a different representation in terms of a zpk-model is used for PES12 which is equivalent to the transfer function definition of PES 11:

$$z = [\,] \qquad p = 0.0 \qquad k = 3.1416 \cdot 10^{-4} \qquad \text{Eq 5-75}$$

5.12.3 Statistical Interpretation

As the 'initial' sources of PES 12 and PES 11 are identical, the same statistical interpretation applies as in section 5.11.3.

5.12.4 Correlation

PES 12 is fully correlated with PES 11, as they basically represent the same source.

5.13 PES 13: Cryocooler Micro-Vibrations

5.13.1 Description

This PES represents the impact of micro-vibrations induced by the cryogenic cooling device on the pointing error of.

5.13.2 Model

As micro-vibrations are dominated by periodic components, the PES can be modelled as RP type Periodic which is defined by frequency and amplitude. From measurements, the amplitudes of the micro-vibration force at a fundamental frequency f_{13} = 57.5 Hz and higher harmonics is given (see Figure 5-11). With these discrete values, the PES can be modelled as:

$$\boldsymbol{\alpha}_{13} = \begin{bmatrix} P(\mathbf{f}_{13}, \mathbf{A}_{13,x}) \\ P(\mathbf{f}_{13}, \mathbf{A}_{13,y}) \\ P(\mathbf{f}_{13}, \mathbf{A}_{13,z}) \end{bmatrix} \text{ mN} \qquad \text{Eq 5-76}$$

where $\mathbf{f}_{13}$ a vector consisting of the fundamental frequency f_{13} and the considered harmonics (i.e. multiples of f_{13}). $\mathbf{A}_{13,ax}$ represents the vector of the respective amplitudes for each axis `ax`. For the sake of simplicity, only the first two harmonics will be considered for the PointingSat example, i.e.:

$$\boldsymbol{\alpha}_{13} = \begin{bmatrix} P(\mathbf{f}_{13}, \mathbf{A}_{13,x}) \\ P(\mathbf{f}_{13}, \mathbf{A}_{13,y}) \\ P(\mathbf{f}_{13}, \mathbf{A}_{13,z}) \end{bmatrix} \text{mN} = \begin{bmatrix} P([57.5,115]\text{Hz}, [180,160]) \\ P([57.5,115]\text{Hz}, [180,160]) \\ P([57.5,115]\text{Hz}, [60,80]) \end{bmatrix} \text{ mN} \qquad \text{Eq 5-77}$$

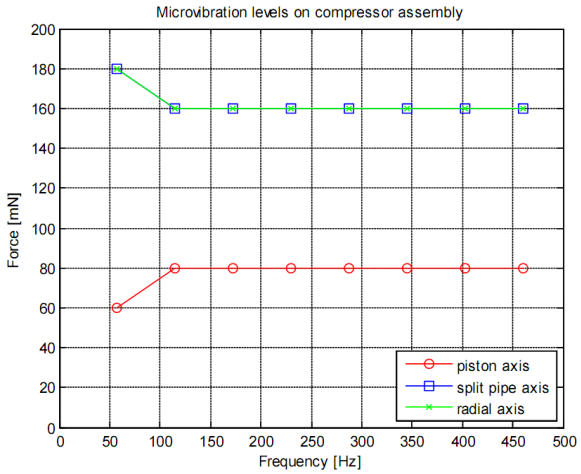

Figure 5-11: Cryocooler micro-vibration levels at distinct frequencies

5.13.3 Statistical Interpretation

The following statements about the statistical interpretation are in line with the descriptions given in Table 8-4 in [AD1], as the amplitudes are discrete and have no ensemble distribution

Generally the statistical interpretation is not applied at PES level for RP type PES but at PEC level (see section 5.3.3), i.e. the $\mathbf{A}_{13,i}$ in the following subsections would have to replaced by resulting $\mathbf{A}'_{13,i}$ after system transfer (in case any system transfer would be present in AST-2).

Note: Using PEET the user would only have to define the PES of RP type Periodic, further interpretation is performed automatically for the user-selected statistical interpretation.

5.13.3.1 Temporal

- **RPE and APE:**

In case of a description in terms of RP type Periodic, the PES can be described by a bimodal distribution characterized by discrete amplitudes, i.e.

$$\boldsymbol{\alpha}_{13,\text{temporal}} = \begin{bmatrix} \text{BM}(\mathbf{A}'_{13,x}) \\ \text{BM}(\mathbf{A}'_{13,y}) \\ \text{BM}(\mathbf{A}'_{13,z}) \end{bmatrix} \text{rad} \qquad \text{Eq 5-78}$$

5.13.3.2 Ensemble

- **APE:**

In case of a description in terms of RP type Periodic, the PES would have to be described by worst case amplitudes at each frequency. With the discrete amplitudes this collapses again simply to:

$$\boldsymbol{\alpha}_{13,\text{ensemble}} = \begin{bmatrix} \mathbf{A}'_{13,\text{max},x} \\ \mathbf{A}'_{13,\text{max},y} \\ \mathbf{A}'_{13,\text{max},z} \end{bmatrix} \text{rad} = \begin{bmatrix} \mathbf{A}'_{13,x} \\ \mathbf{A}'_{13,y} \\ \mathbf{A}'_{13,z} \end{bmatrix} \text{rad} \qquad \text{Eq 5-79}$$

5.13.3.3 Mixed

- **PRE and APE:**

As the ensemble behaviour is constant for this PES, the mixed statistical interpretation corresponds to the temporal one, i.e.

$$\boldsymbol{\alpha}_{13,\text{mixed}} = \boldsymbol{\alpha}_{13,\text{temporal}} \qquad \text{Eq 5-80}$$

5.14 PES Summary

The following table summarizes the types and description for the different PES of PointingSat.

Table 5-1: PES Summary

PES No.	Type	Description
1	CRV	Mechanical alignment between payload and star tracker
2	CRV	Misalignment between payload and star tracker due to launch effects
3	RP (PSD)	Force noise of single thruster
4	CRV	Star tracker measurement bias
5	RP (Covariance)	Star tracker temporal measurement noise (temperature/orientation independent part)
6	RP (PSD)	Star tracker FOV and pixel noise
7	RP (PSD)	Rate noise of gyro assembly
8	CRV, Drift, RP(PSD)	Time series of environmental disturbances on satellite body
9	RP (Periodic)	Periodic part of thermo-elastic distortion affecting the alignment between payload to star tracker
10	RV	Random part of thermo-elastic distortion affecting the alignment between payload to star tracker
11	RP (PSD)	Thermal stability effect on star tracker measurement
12	RP (PSD)	Thermal stability effect on focal point stability
13	RP (Periodic)	Cryocooler induced micro-vibrations

6 Transfer Analysis (AST-2)

This section covers the transfer analysis of the PES according to AST-2 in [AD1]. The first subsection describes the system transfer for each PES in general, the second subsection defines the applied system models.

6.1 PES System Transfers

6.1.1 PES1: Mechanical Payload and Star Tracker Alignment

As the measurement error knowledge is provided with respect to the satellite body axes (coinciding with the nominal payload axes), no further system transfer is required, i.e. PES 1 directly represents a PEC.

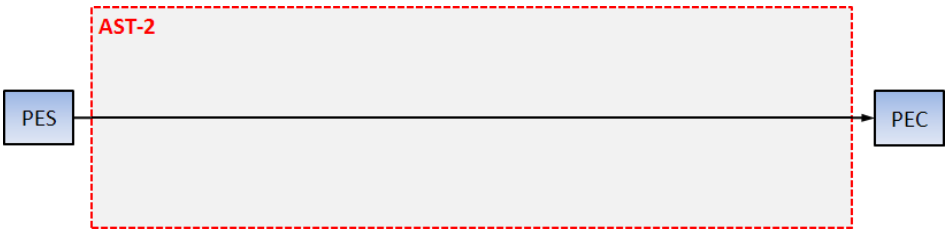

Figure 6-1: System transfer of PES 1 (according to AST-2 in [AD1]).

6.1.2 PES2: Star Tracker to Payload Alignment after Launch

As the payload to star tracker misalignment directly describes relevant error information, no further system transfer is required, i.e. PES 2 directly represents a PEC.

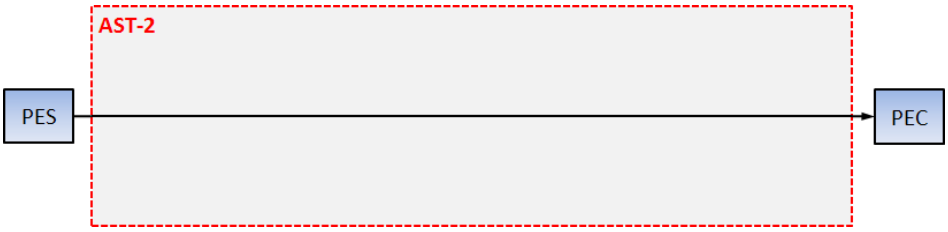

Figure 6-2: System transfer of PES 2 (according to AST-2 in [AD1]).

6.1.3 PES3: Thruster Noise

As PES 3 only represents one single actuator of the whole assembly, the force noise of one individual thruster has to be converted to a torque noise from the entity of thrusters first. This is done via the actuation matrix describing the orientation and position of all actuators in the body frame. The resulting torque noise is then treated as disturbance input η_d on the satellite plant in the closed-loop feedback system (see section 6.2.8). It is thus turned into a PEC by applying the closed-loop transfer function matrix from disturbance input η_d to the control variable y (representing the pointing angles).

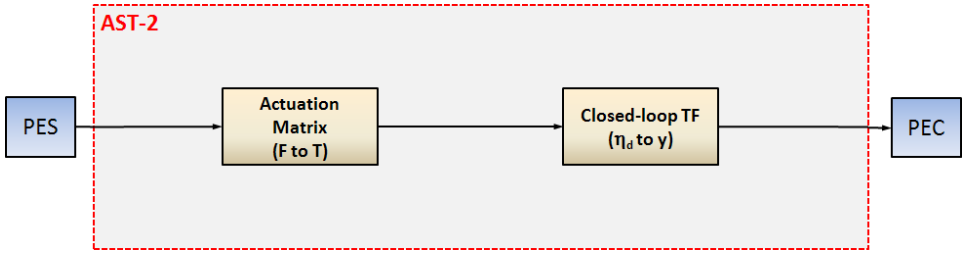

Figure 6-3: System transfer of PES 3 (according to AST-2 in [AD1]).

6.1.4 PES 4: Star Tracker Bias

As the nominal sensor (more precisely the camera head) frame has a different orientation compared to the satellite body axes, PES 4 first has to be fed through a CTF in order to represent a PEC in the correct frame.

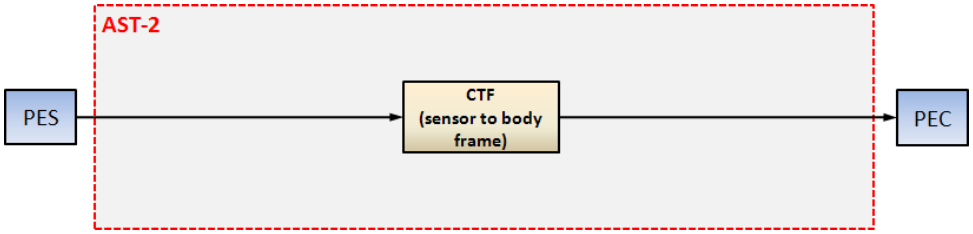

Figure 6-4: System transfer of PES 4 (according to AST-2 in [AD1]).

6.1.5 PES 5: Star Tracker Noise (Temporal)

The PES itself describes one part of the unprocessed measurement noise of the star tracker in its sensor frame. Thus, it first has to be expressed in body axes via a coordinate transformation. Then the converted noise is further processed via an gyro-stellar estimator (Kalman Filter) for further noise reduction. The filtered noise (more precisely the attitude estimation error) is finally treated as measurement error input η_m in the closed-loop feedback system (see section 6.2.8). It is thus turned into a PEC by applying the closed-loop transfer function matrix from measurement noise η_m to the control variable y (representing the pointing angles).

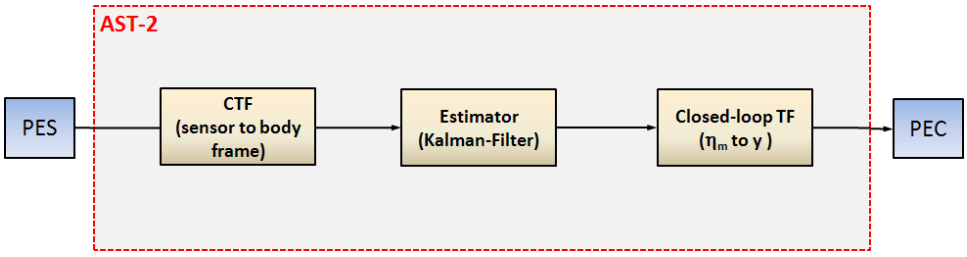

Figure 6-5: System transfer of PES 5 (according to AST-2 in [AD1]).

6.1.6 PES 6: Star Tracker FOV and Pixel Spatial Errors

The PES itself describes another part of the unprocessed measurement noise of the star tracker in its sensor frame. Thus, it first has to be expressed in body axes via a

coordinate transformation. Then the converted noise is further processed via an gyro-stellar estimator (Kalman Filter) for further noise reduction. The filtered noise (more precisely the attitude estimation error) is finally treated as measurement error input η_m in the closed-loop feedback system (see section 6.2.8). It is thus turned into a PEC by applying the closed-loop transfer function matrix from measurement error η_m to the control variable y (representing the pointing angles).

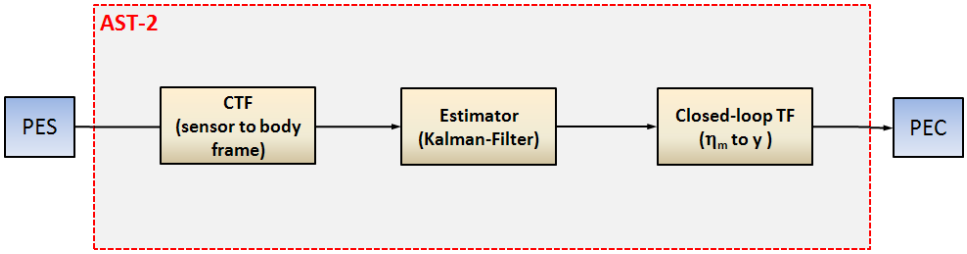

Figure 6-6: System transfer of PES 6 (according to AST-2 in [AD1]).

6.1.7 PES 7: Gyro Noise

The PES itself describes the unprocessed measurement noise of the gyro assembly. This noise is first processed via an estimator (Kalman Filter) for further noise reduction. The filtered noise then treated as measurement error input η_m in the closed-loop feedback system (see section 6.2.8). It is thus turned into a PEC by applying the closed-loop transfer function matrix from measurement error η_m to the control variable y (representing the pointing angles).

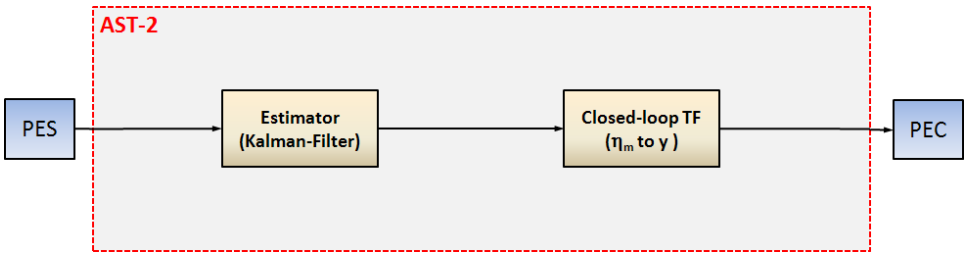

Figure 6-7: System transfer of PES 7 (according to AST-2 in [AD1]).

6.1.8 PES 8: Environmental disturbances

The environmental torques act on the satellite body and are counteracted by the AOCS. Using the common description of a closed-loop feedback system (see section 6.2.8), PES 8 acts as a disturbance input η_d on the satellite plant. It is thus turned into a PEC by applying the closed-loop transfer function matrix from η_d to the control variable y (representing the pointing angles).

.

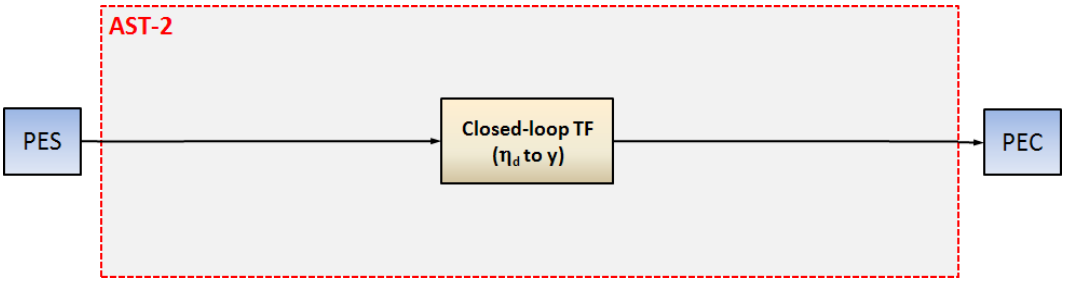

Figure 6-8: System transfer of PES 8 (according to AST-2 in [AD1]).

6.1.9 PES 9: Thermo-Elastic Distortion (Periodic Part)

As the thermo-elastic distortion between payload and star tracker directly affects the pointing error, no further system transfer is required, i.e. PES 9 directly represents a PEC.

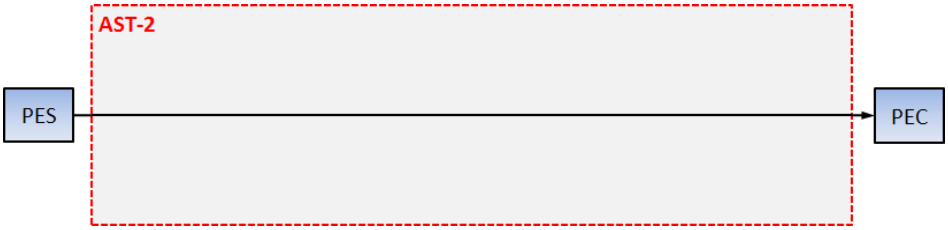

Figure 6-9: System transfer of PES 9 (according to AST-2 in [AD1]).

6.1.10 PES 10: Thermo-Elastic Distortion (Random Part)

As the thermo-elastic distortion between payload and star tracker axes directly affects the pointing error, no further system transfer is required, i.e. PES 10 directly represents a PEC.

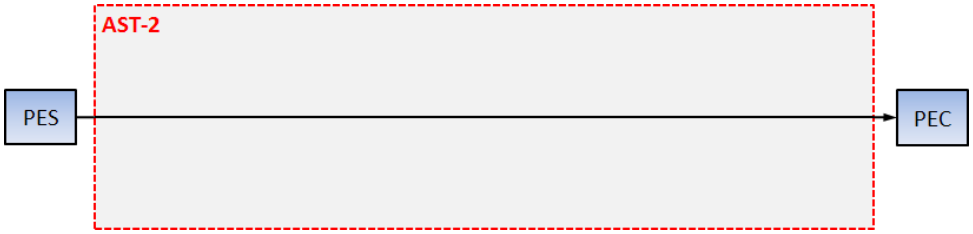

Figure 6-10: System transfer of PES 10 (according to AST-2 in [AD1]).

6.1.11 PES11: Thermal Stability Effect on Star Tracker

The PES describes the temperature stability at a location different from the required one. For that reason, the first step is to apply a thermal filter that describes the temperature transfer behaviour from the reference point on the optical bench interface to the star tracker camera head/detector. The converted temperature stability is input for model

describing the thermal noise impact on the detector, i.e. the induced measurement noise in the sensor frame. This noise has to be expressed subsequently in the body frame before it is further processed in the attitude estimator. The residual noise is finally treated as measurement error input η_m in the closed-loop feedback system (see section 6.2.8). It is thus turned into a PEC by applying the closed-loop transfer function matrix from measurement error η_m to the control variable y (representing the pointing angles).

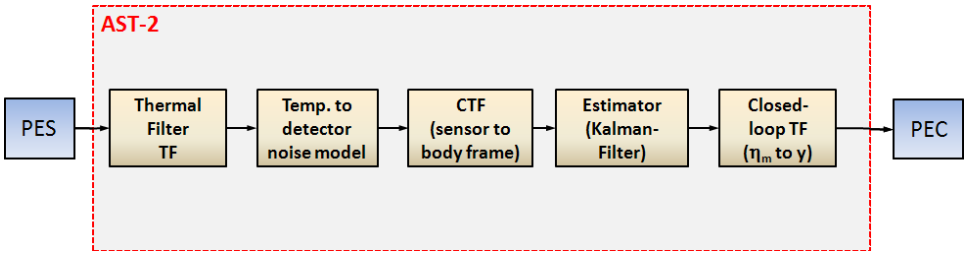

Figure 6-11: System transfer of PES 11 (according to AST-2 in [AD1]).

6.1.12 PES12: Thermal Stability Effect on Payload

Similar to PES 11 this PES describes the temperature stability at a location different from the required one. For that reason, the first step is to apply a thermal filter that describes the temperature transfer behaviour from the reference point on the optical bench interface to the structural parts affecting the focal point. The resulting temperature stability is input for a model describing the distortion impact of thermal noise on the focal point.

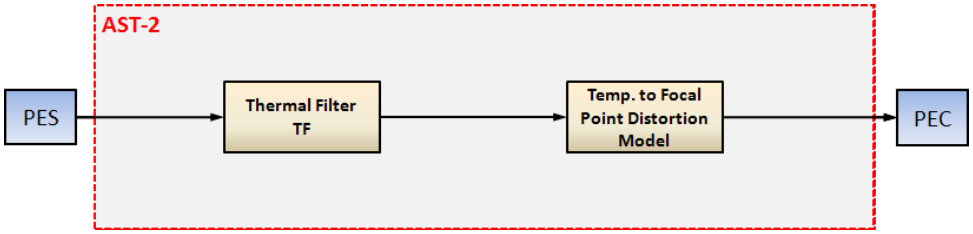

Figure 6-12: System transfer of PES 12 (according to AST-2 in [AD1]).

6.1.13 PES 13: Cryocooler Micro-Vibrations

The PES describes the micro-vibrations at force level at the location of the cryocooler compressor. To convert these forces into an equivalent pointing error, the PES is input to a model representing the structural response of the satellite system in terms of pointing impact.

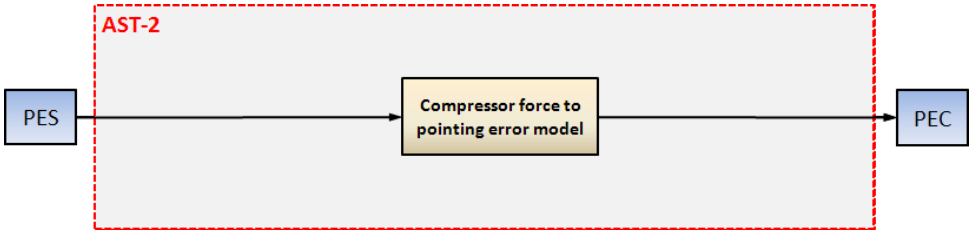

Figure 6-13: System transfer of PES 13 (according to AST-2 in [AD1]).

6.2 Transfer Model Definition

This chapter describes the applied models for the system transfer of the PES presented in the previous subsection (see also overview in Figure 6-19). The models are partially very simplified at the current state and might be replaced in case more detailed descriptions become available.

6.2.1 Thruster actuation matrix

The force noise (PES3) is available for a single thruster along its thrust direction in terms of a PSD. To convert the (identical) individual noise to an equivalent torque noise of the whole set of N_{thr} thrusters, an actuation matrix A_{thr} of size N_{thr} x 3 is necessary which implicitly includes the position and orientation of each thrusters with respect to the spacecraft body frame. For the PointingSat example using 10 actuators, this actuation matrix is given by:

$$\mathbf{A}_{thr} = \begin{bmatrix} 1.9445 & 0 & 0 \\ -1.9445 & 0 & 0 \\ 1.9445 & 0 & 0 \\ -1.9445 & 0 & 0 \\ 0 & 1.8385 & 0 \\ 0 & -1.8385 & 0 \\ 0 & -0.4000 & -1.5000 \\ 0 & 0.4000 & 1.5000 \\ 0 & 0.4000 & -1.5000 \\ 0 & -0.4000 & 1.5000 \end{bmatrix} \text{ m} \qquad \text{Eq 6-1}$$

Using PEET the user would define this matrix by using the dynamic system block “Mapping Matrix’, defining an input number of 10 (according to N_{thr}).

6.2.2 Coordinate Transformation (star tracker to body frame)

As star tracker frame and body frame are not aligned, transformation of the star tracker noise is necessary. For the PointingSat example, the orientation of the star tracker frame

with respect to the spacecraft body is given by the Euler angles (using the common roll-pitch-yaw description):

$$\Phi = 0 \text{ deg}$$

$$\Theta = 90 \text{ deg}$$

$$\Psi = 180 \text{ deg}$$

The underlying mounting direction is selected such that the star tracker boresight axis is anti-parallel to the telescope body axis to exclude large coupling of the less accurate sensor axis to telescope pointing. The transformation is realized in PEET using the static system 'Coordinate Transformation' and defining the three Euler angles with the desired rotation sequence (3-2-1 in this case) defining:

$$\mathbf{T} = \begin{bmatrix} c\theta \cdot c\psi & c\theta \cdot s\psi & -s\theta \\ -c\Phi \cdot s\psi + s\Phi \cdot s\theta \cdot c\psi & c\Phi \cdot c\psi + s\Phi \cdot s\theta \cdot s\psi & s\Phi \cdot c\theta \\ s\Phi \cdot s\psi + c\Phi \cdot s\theta \cdot c\psi & -s\Phi \cdot c\psi + c\Phi \cdot s\theta \cdot s\psi & c\Phi \cdot c\theta \end{bmatrix} \quad \text{Eq 6-2}$$

where s and c abbreviate sine and cosine respectively.

6.2.3 Gyro-Stellar Estimator

Rate measurements of the gyroscopes and attitude measurements from the star tracker are filtered using a gyro-stellar estimator (basically a fixed-gain Kalman filter) to obtain an improved attitude estimate as well as an estimate of the drift bias on the rate measurement.

Assuming a single-axis filter for each of the three body axes, the transfer function matrix for the estimation errors on each axis (which are fed to the PD controller) is given by (see [RD2]):

$$\begin{bmatrix} \tilde{\varphi} \\ \tilde{B} \end{bmatrix} = \frac{1}{s^2 + K_1 s + K_2} \begin{bmatrix} (K_1 s + K_2) n_{Str} + s\, n_{gyro} + B_{gyro} \\ -K_2 s\, n_{Str} + K_2\, n_{gyro} - (s + K_1) B_{gyro} \end{bmatrix} \quad \text{Eq 6-3}$$

where axis indices have been omitted. The inputs to the gyro-stellar estimator block are thus the star tracker noise contributions (from PES 4,5, 6 and 11) combined in n_{str} and the gyro noise n_{gyro} from PES7 (that implicity includes drift bias noise as rate random walk contribution, i.e. the B_{gyro} input is not used for this setup. If this 'combined' modelling is not available/desired, the user could specify the drift bias as individual PES and feed it to the respective input).

The Kalman gains[2] for the different axes are given by:

$$\mathbf{K}_1 = \begin{bmatrix} K_{1x} \\ K_{1y} \\ K_{1z} \end{bmatrix} = \begin{bmatrix} 0.2 \\ 0.2 \\ 0.2 \end{bmatrix} \quad \text{Eq 6-4}$$

[2] Note that K_1 and K_2 correspond to the gains K_p and K_d in the block mask dialog.

$$\mathbf{K}_2 = \begin{bmatrix} K_{2,x} \\ K_{2,y} \\ K_{2,z} \end{bmatrix} = \begin{bmatrix} 0.005 \\ 0.005 \\ 0.003 \end{bmatrix} \qquad \text{Eq 6-5}$$

6.2.4 Thermal Filters

For PES 11 and 12 only the thermal stability at a measurement point different from the required ones is available. The thermal filter models describe the transfer of the temperature stability via the spacecraft structure to the desired locations, namely the star tracker detector and payload telescope structure. Generally this information will be computed with complex FEM models.

For the PointingSat example, it is assumed that an approximate solution can be extracted from the complex model which can be characterized by a simple transfer function with low-pass behaviour (illustrated in Figure 6-14):

$$TF_{thermal,1} = \frac{0.01257}{s + 0.01257} \qquad \text{Eq 6-6}$$

$$TF_{thermal,2} = \frac{3.142 \cdot 10^{-3}}{s + 3.142 \cdot 10^{-3}} \qquad \text{Eq 6-7}$$

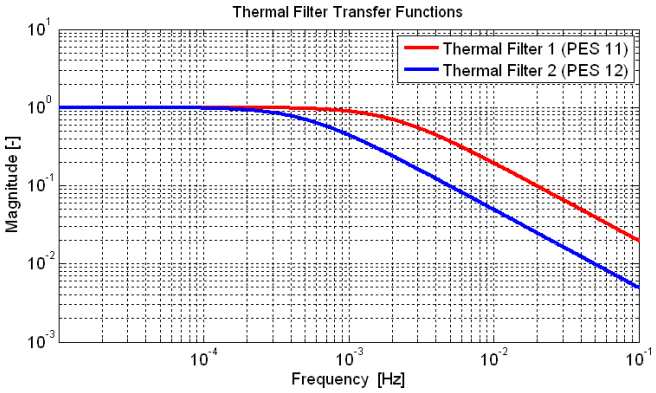

Figure 6-14: Thermal filter transfer functions for transfer of PES 11 and PES 12

This model can be realized in PEET by feeding the PES by a dynamic system block and defining above transfer functions on all main diagonals.

6.2.5 Temperature Stability to Detector Noise Model

Due to the lack of a more sophisticated model for the system transfer of PES 11 at current state, the impact of temperature stability on the noise of the star tracker is realized in a very simplified way.

The underlying assumption is that the temperature changes have approximately a linear effect on the detector due to thermal expansion. Some structural ‘damping’ of the temperature fluctuations generally exist which can be considered already treated by the

applied thermal filters (section 6.2.4). The 'remainder' is then a static gain which gets directly mapped into attitude errors via a certain scaling factor.

This model is realized in PEET using a static system with the respective conversion gains $K_{11,ax}$ on the main diagonal:

$$\begin{bmatrix} K_{11,x} & 0 & 0 \\ 0 & K_{11,y} & 0 \\ 0 & 0 & K_{11,z} \end{bmatrix} \frac{\text{arcsec}}{\text{K}} = \begin{bmatrix} 1.34 & 0 & 0 \\ 0 & 1.34 & 0 \\ 0 & 0 & 0.65 \end{bmatrix} \frac{\text{arcsec}}{\text{K}} \qquad \text{Eq 6-8}$$

6.2.6 Temperature Stability to Focal Point Distortion Model

As for the system transfer of PES 11, no sophisticated model for the system transfer of PES 12 is available.

Assuming again the structural damping to be already covered by the thermal filter in section 6.2.4 and an approximately linear impact due to thermal expansion, the effect of the focal point distortion can be realized once more by a static system with conversion gains $K_{12,ax}$ on the main diagonal of the block:

$$\begin{bmatrix} K_{12,x} & 0 & 0 \\ 0 & K_{12,y} & 0 \\ 0 & 0 & K_{12,z} \end{bmatrix} \frac{\text{arcsec}}{\text{K}} = \begin{bmatrix} 0.89 & 0 & 0 \\ 0 & 1.16 & 0 \\ 0 & 0 & 1.19 \end{bmatrix} \frac{\text{arcsec}}{\text{K}} \qquad \text{Eq 6-9}$$

6.2.7 Compressor Force to Pointing Error Conversion

As for the temperature stability related effects, some kind of FEM model would be required for a detailed computation of the compressor forces transfer of PES 13 via the structure to an equivalent pointing error. For the PointingSat example it is assumed that this transfer behaviour can be sufficiently approximated transfer function of a spring-damper-system that accounts for the structural damping implicitly scaled by an additional conversion factor describing the relation between force and pointing, i.e.

$$TF_{structure} = \frac{K_{13}\omega_0^2}{s^2 + 2\zeta\omega_0 s + \omega_0^2} \qquad \text{Eq 6-10}$$

Assuming a damping factor ζ=0.1, a structure eigenfrequency of 10 Hz and a conversion factor K_{13} = 1.6 arcsec/N for the PointingSat example, the corresponding transfer function (identical for all axes) is shown in Figure 6-15 below.

The realization in PEET requires then the definition of above transfer function on the main diagonals of a dynamic system block.

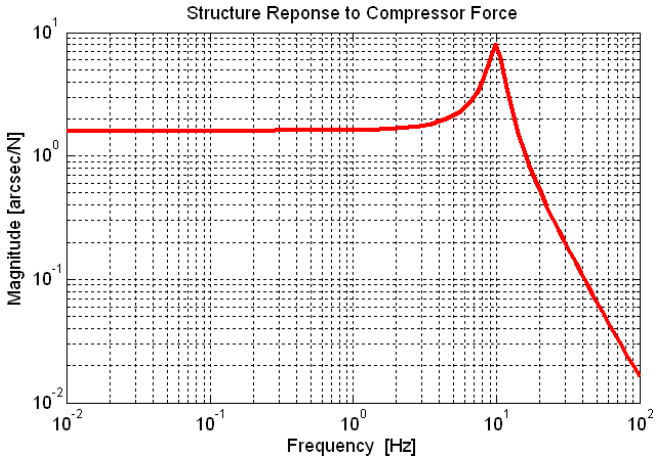

Figure 6-15: Structure Response to force loads

6.2.8 Feedback Loop

Generally, any feedback system required for the system transfer could be realized by defining the respective closed-loop transfer function for each PES in a standard PEET 'Dynamic System' block. Assume that multiple PES have to be fed through the same feedback system but at different 'input locations' of the loop. In this case multiple 'Dynamic System' blocks are required and a modification of parameters in the feedback system would lead to a manual re-computation of the transfer function by the user with subsequent editing of multiple blocks.

To avoid such effort, the 'Feedback System' block in PEET block can be used to modify parameters directly with automatic update of the underlying closed-loop transfer function.

6.2.8.1 Satellite plant model

The satellite plant is assumed to be a rigid body which is fully defined by its inertia for the pointing error evaluation purpose. Neglecting couplings between the body axes for the PointingSat example, the transfer function of the satellite plant (from torque to attitude) for axis `ax` is simply given by:

$$G = TF_{plant,ax} = \frac{1}{\Theta_{ax,ax}\, s^2} \qquad \text{Eq 6-11}$$

where $\Theta_{ax,ax}$ is the main diagonal element of the inertia tensor for axis `ax`. The inertia tensor for PointingSat is assumed as:

$$\boldsymbol{\Theta} = \begin{bmatrix} 4600 & 0 & 0 \\ 0 & 4300 & 0 \\ 0 & 0 & 1800 \end{bmatrix} \text{kgm}^2 \qquad \text{Eq 6-12}$$

6.2.8.2 Attitude controller

For the purpose of PointingSat, a simple SISO PD controller is used for attitude control separately for each body axes:

$$TF_{ctrl.ax} = K_{P,ax}\varphi_{ax} + K_{D,ax}\omega_{ax} \quad \text{Eq 6-13}$$

$K_{P,ax}$ and $K_{D,ax}$ denote the proportional and derivative gains for the respective axis. Generally φ_{ax} describes the difference between desired attitude and attitude estimate from the gyro-stellar estimator (around axis `ax`) and ω_{ax} the difference between desired rate and measured rate around (around axis `ax`) corrected by the bias estimate from the gyro-stellar estimator, i.e. (axis index omitted):

$$\varphi = \varphi_{ref} - \varphi_{est} = \varphi_{ref} - (\varphi_{real} + \tilde{\varphi}) \quad \text{Eq 6-14}$$

$$\omega = \omega_{ref} - \omega_{est} = \omega_{ref} - (\omega_{real} + \omega_{noise} + B_{real} - (B_{real} + \tilde{B})) \quad \text{Eq 6-15}$$

As only error signals are relevant for the scope of pointing error analysis, it is not the 'complete' signal which has to be fed to the controller in the feedback block. These required signals are represented by the attitude and drift bias estimation error only, which are the output of the gyro-stellar estimation block (denoted with a "~" in the transfer functions in section 6.2.3) and the rate noise from PES 7:

$$\varphi = -\tilde{\varphi} \quad \text{Eq 6-16}$$

$$\omega = -\omega_{noise} + \tilde{B} \quad \text{Eq 6-17}$$

For the PointingSat example, the following controller gains are used and specified in the 'PID Controller' tab of the feedback block assuming a 0.08 Hz bandwidth of the attitude control:

$$\mathbf{K}_P = \begin{bmatrix} K_{P,x} \\ K_{P,y} \\ K_{P,z} \end{bmatrix} = -\begin{bmatrix} 581.23 \\ 543.97 \\ 227.71 \end{bmatrix} \quad \text{Eq 6-18}$$

$$\mathbf{K}_I = \begin{bmatrix} K_{I,x} \\ K_{I,y} \\ K_{I,z} \end{bmatrix} = \begin{bmatrix} 0 \\ 0 \\ 0 \end{bmatrix} \quad \text{Eq 6-19}$$

$$\mathbf{K}_D = \begin{bmatrix} K_{D,x} \\ K_{D,y} \\ K_{D,z} \end{bmatrix} = -\begin{bmatrix} 1976.2 \\ 1849.5 \\ 774.2 \end{bmatrix} \quad \text{Eq 6-20}$$

The overall transfer function of the SISO-PID controller for each axis is given by:

$$K = K_P + \frac{K_I}{s} + K_D s \qquad \text{Eq 6-21}$$

6.2.8.3 Loop structure

If the PID controller input would only be dependent on a single source (i.e. attitude estimation error from GSE only), the setup of the simple loop structure shown in Figure 6-16 below would be sufficient (undefined sub-blocks in the 'Feedback System' block have default unity transfer).

It consists of a PID controller K from and a rigid body plant model G (with the parameters defined in the previous subsections) with PES acting on the disturbance (η_d) and measurement error (η_m) inputs and affecting the pointing output y (=φ in this case).

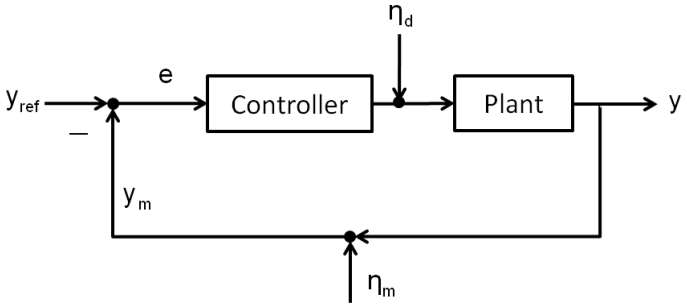

Figure 6-16: Feedback loop structure (attitude noise input only)

For the PointingSat example a more complex loop scheme is required as the controller input not only comprises attitude information as single source, but also rate information. Generally, this would require an inner loop for the rate feedback (see figure below) while nested loops are not directly supported by PEET.

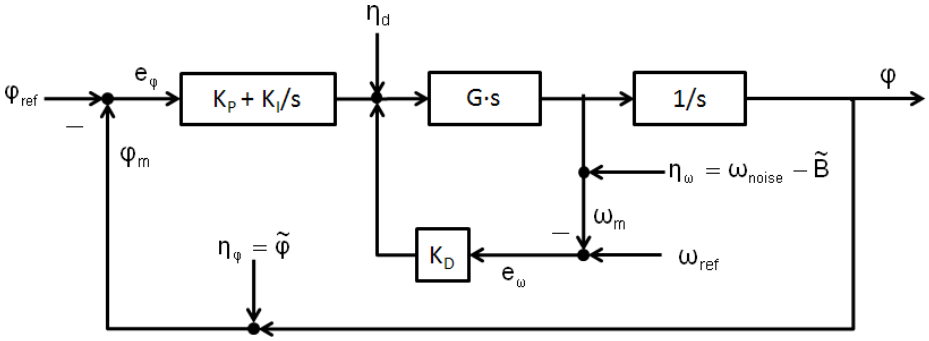

Figure 6-17: Feedback loop structure (with attitude and rate noise input)

However, loop block manipulation (inner loop reduction, moving summing junctions, cascading blocks, etc.) leads to totally equivalent representations of above loop scheme which allow a realization in PEET. Two possible realizations using prefilters (dynamic

system blocks) for the individual noise inputs are shown in Figure 6-18. Realization a) treats all input noises as artificial disturbance noise while realization b) which is available as container in the block database of PEET preserves the 'physical' inputs.

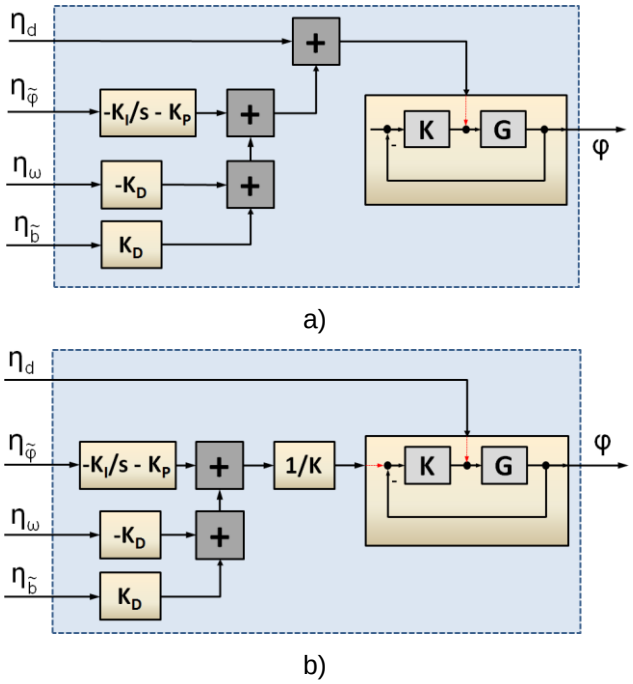

Figure 6-18: Equivalent realizations

6.3 PointingSat realization in the PEET

There are multiple ways of setting up the previously described pointing system in PEET. One possible realization of the overall PES and system transfer is shown below which is the most 'compact' one in terms of block usage. It corresponds to the system setup in the PointingSat.peet example delivered with the software (located in `peetroot`\examples).

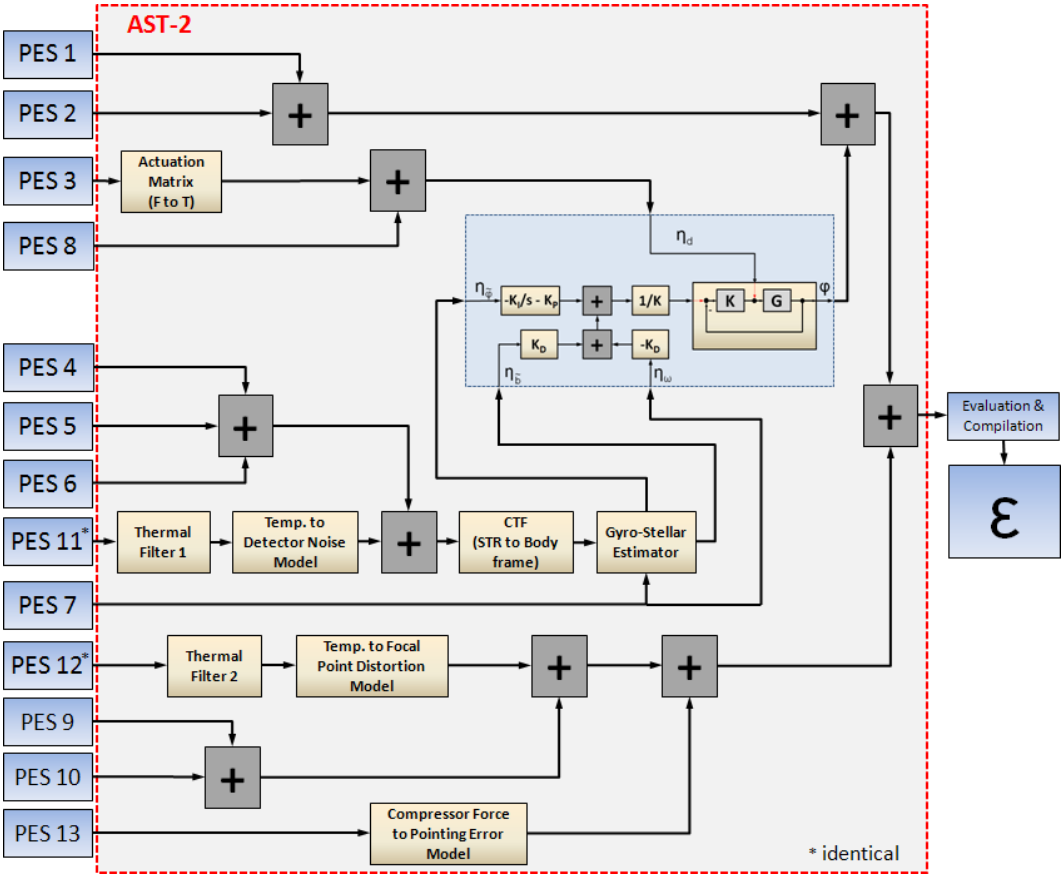

Figure 6-19: System realization in PEET used for PointingSat

An alternative setup is shown in Figure 6-20. It follows a 'parallel' approach with one final summation after all system transfers. This setup could simplify the determination of the driving PES, as the individual contributions can directly be compared at the input ports of the summation block in the PEET tree-view. A possible disadvantage is multiple use of identical blocks which complicates quick changes of the system structure or may result in larger computation times due to the larger number of signals to be computed.

Generally, a 'mixed' approach, i.e. setting up several levels of parallel paths + summation block allows grouping of device or subsystem levels (up to the top-level error) with quick error evaluation on each level by analysing the input ports of the respective summation block. This is schematically depicted in Figure 6-21.

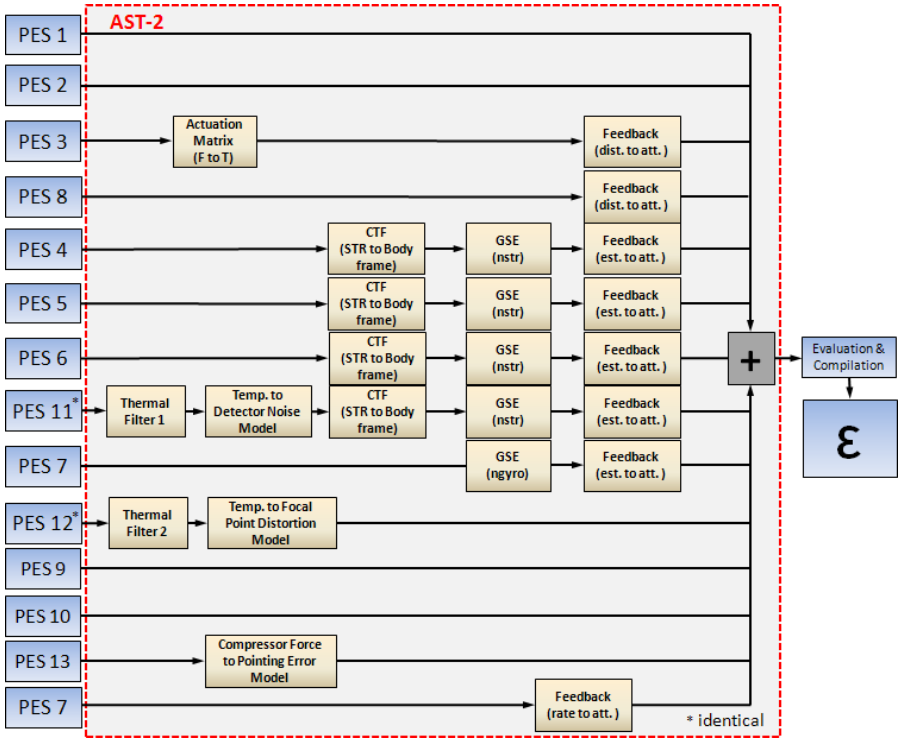

Figure 6-20: Alternative system realization: 'Parallel approach'

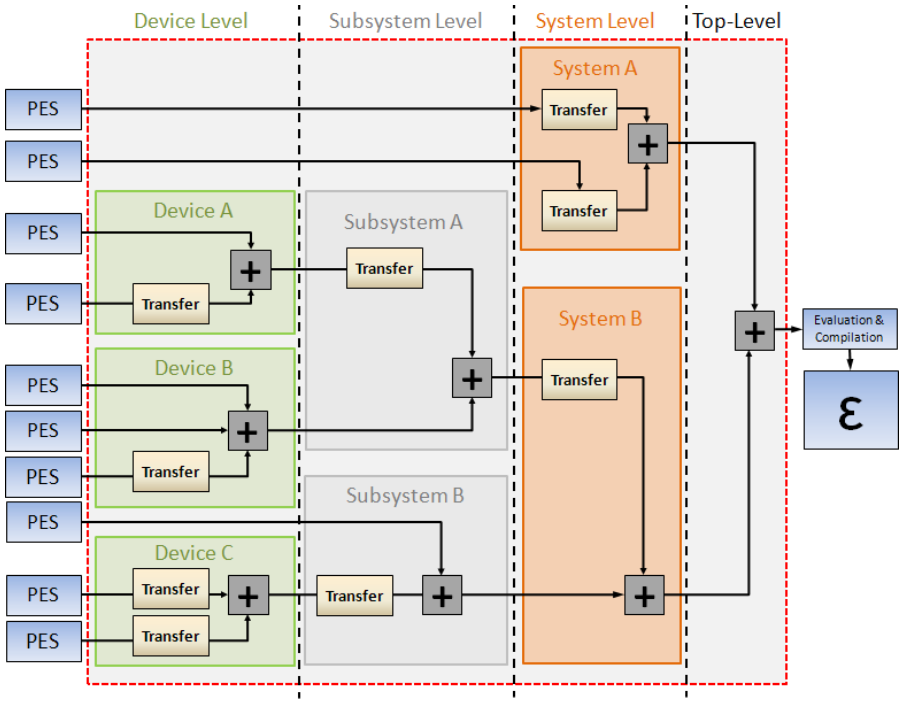

Figure 6-21: Grouping on different system level (schematic)

7 Pointing Error Index Contribution (AST-3)

This section briefly describes the time-windowed pointing error index contribution analysis for the PointingSat example in accordance to AST-3 in [AD1]. This step is mainly related to the application of the pointing error metrics which are dependent on error index under consideration.

For all PES (more precisely PEC at this point) which are described as random process this is realized via pointing error metric weighting functions (Table 10-3 in [AD1]). In case of a time-random variable description of the PEC, the tables in appendix B of [AD2] are applied. While the latter represents only an approximation of the error contribution, the random process analysis is exact. Consequently, random process description of the PES/PEC should be preferred when sufficient data is available.

The contribution analysis is done automatically in PEET for all time-random PEC (as the time-constant ones do not contribute by definition).

AST-3 includes also the statistical interpretation of PEC which originate from RP type PES. This interpretation at PEC level is already highlighted in the statistical interpretation subsections for the respective PES in section 5 for compactness.

8 Pointing Error Evaluation (AST-4)

This section describes the results of pointing error evaluation for the PointingSat example according to AST-4 in [AD1]. It consists of user-defined assumptions on the correlation of the different PEC, their summation per index and the level of confidence evaluation of the resulting sum.

8.1 Correlation

According to [AD1], assumptions on the correlation between different PES are required to perform the final pointing error evaluation. In PEET, correlation is defined on PES level in the respective dialog of the PES blocks (correlation between axes) and in the global settings (correlation between PES).

The ‘evolution’ of the correlation through the system transfer (e.g. cross-coupling of axes, addition of signals, etc.) is automatically tracked by the software. The following chapters summarize the assumptions on the initial correlation state of the different PES.

8.1.1 PES 1: Mechanical Payload and Star Tracker Alignment

As the alignment measurement for the payload telescope and the star tracker is based on theodolite measurements, it is conceivable that the knowledge errors of three axes are not independent from each other. For that reason, knowledge errors of the PES are assumed to be fully correlated among the different axes.

In addition PES 1 is assumed to be fully uncorrelated with all other PES as they have no 'physical' link to the payload and star tracker integration process.

8.1.2 PES 2: Star Tracker to Payload Alignment after Launch

As the launch can be treated as a single event, there is no correlation between PES 2 and other PES. As no information is available for the behaviour between different axes of PES 2, no correlation is assumed in this case as well.

8.1.3 PES 3: Thruster Noise

As this PES consists of only one component, no correlation between axes can be specified. In addition, PES 3 is assumed to be uncorrelated with other PES as they have no 'physical commonalities'.

Note that when applying the actuation matrix, PES 3 is implicitly split into multiple identical PES dependent on the number of involved thrusters. The correct correlation (cross-coupling) state on torque axes level is directly defined via the actuation matrix itself.

8.1.4 PES 4: Star Tracker Bias

As the star tracker bias results from a combination of different effects (calibration and launch effects) where no further information is available, it is assumed that the bias knowledge errors of different axes are uncorrelated.

In addition PES 4 is assumed to be fully uncorrelated with all other PES as they have no 'physical' link to other PES.

8.1.5 PES 5: Star Tracker Noise (Temporal)

As no information about the axes cross-coupling is available, the off-diagonal terms of the covariance matrix are zero, i.e. no correlation between PES 5 axes. Due to the sensor intrinsic properties of the noise, there is no correlation with other PES as well.

8.1.6 PES 6: Star Tracker FOV and Pixel Spatial Errors

As no information about the axes cross-coupling is available, the off-diagonal terms of the spectral density matrix are zero, i.e. no correlation between PES 6 axes. Due to the sensor intrinsic properties of the noise, there is no correlation with other PES as well.

8.1.7 PES 7: Gyro Noise

Although the information of the body rate is obtained from identical sensors in the gyro assembly, no correlation between the different axes of PES 7 is assumed (as each of the sensors is aligned with the one of the body axis and no 'mixing' of measurement from different gyros is required to obtain a single body axis rate component). In addition PES 7 is assumed to be fully uncorrelated with other PES.

8.1.8 PES 8: Environmental Disturbances

No correlation between PES 8 and other PES is assumed. The information about correlation between different axes of PES 8 is fully available from the time series. Thus it is possible to set up the full power spectral density matrix as follows:

$$\mathbf{n}_{T,8} = \begin{bmatrix} PSD_{8,xx} & PSD_{8,xy} & PSD_{8,xz} \\ PSD_{8,yx} & PSD_{8,yy} & PSD_{8,yz} \\ PSD_{8,zx} & PSD_{8,zy} & PSD_{8,zz} \end{bmatrix} Nm/\sqrt{Hz} \qquad \text{Eq 8-1}$$

Note: This computation is automatically done in PEET when time series PES are available.

8.1.9 PES 9: Thermo-Elastic Distortion (Periodic Part)

As the thermal distortion affects all spatial directions of the spacecraft structure at the same time in the same way (assuming an isotropic thermal expansion coefficient for the relevant structures), the different axes of PES 9 are assumed to be fully correlated. In contrary there is no correlation between PES 9 and other PES.

8.1.10 PES 10 Thermo-Elastic Distortion (Random Part)

As the thermal distortion affects all spatial directions of the spacecraft structure at the same time in the same way (assuming an isotropic thermal expansion coefficient for the relevant structures), the different axes of PES 10 are assumed to be fully correlated. In contrary there is no correlation between PES 10 and other PES.

8.1.11 PES 11 + 12: Thermal Stability Effect on Star Tracker and Payload

Although there is only one non-zero component in the PES, the correlation state between its axis is arbitrary. However, PES 11 is fully correlated with PES 12, as they basically represent the same source.

8.1.12 PES 13: Cryocooler Micro-Vibrations

As the vibration loads affect all spatial directions of the spacecraft structure simultaneously, the different axes of PES 13 are assumed to be fully correlated. In contrary there is no correlation between PES 13 and other PES.

8.2 Summation and Level of Confidence Evaluation

The following subchapters summarize the final pointing error results for the three analysed pointing error indices of the PointingSat example together with the results for all individual signals. The signal (blue) and system numbers (red) correspond to the numbering in the scheme below.

The global frequency evaluation bandwidth used in PEET for all scenarios of the PointingSat example ranges from 10^{-6} Hz to 10^{3} Hz with a resolution of 1000 frequency points.

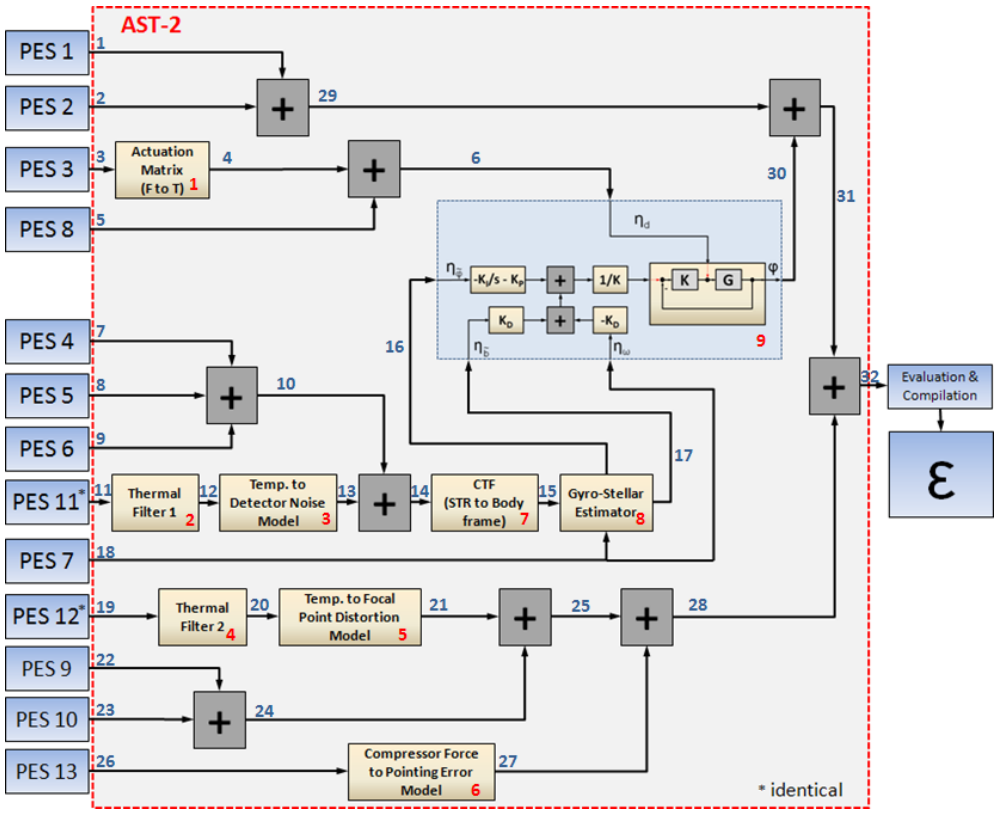

Figure 8-1: Signal and system numbering used in result tables and plots

8.2.1 Scenario 1: APE, ensemble, 3σ (n_p = 3)

Table 8-1 summarizes the pointing error results available from the PEC block tabs in the tree view of PEET. The last three columns contain additional information about the reduction of the total error per axis in % assuming that the respective entry in the x,y,z-data columns of the same row would not be present (i.e. artificially set to zero). Note that as the error evaluation is not linear in all cases, the resulting sum of percentages is not necessarily 100 %.

Table 8-1: Pointing error for scenario 1 (NOTE: data unit is [arcsec])

```
Scenario:  PointingSat (APE, ensemble)
    Data:  Signals (filtered, correlated)
    Unit:  [arcs]
     LoC:  np = 3
```

		x	y	z	x(%)	y(%)	z(%)
Signal Contributions:							
CRV	Mean:	1.85e+001	1.64e+001	1.74e+001	17.3214	24.4315	30.9771
	np x Std:	5.23e+001	3.76e+001	2.86e+001	43.2301	49.6953	44.9389
	Total:	7.08e+001	5.41e+001	4.61e+001	60.5514	74.1268	75.9161
RV	Mean:	4.50e+000	4.50e+000	4.50e+000	4.2214	6.6939	7.9987
	np x Std:	2.60e+000	2.60e+000	2.60e+000	0.0601	0.1326	0.2083
	Total:	7.10e+000	7.10e+000	7.10e+000	4.2815	6.8265	8.2070
D	Mean:	-2.08e-005	-3.22e-005	-1.66e-005	-0.0000	-0.0000	-0.0000
	np x Std:	0.00e+000	0.00e+000	0.00e+000	0.0000	0.0000	0.0000
	Total:	2.08e-005	3.22e-005	1.66e-005	-0.0000	-0.0000	-0.0000
RP	Mean:	2.38e+001	3.54e+000	3.35e+000	22.3464	5.1110	5.9628
	np x Std:	0.00e+000	0.00e+000	0.00e+000	0.0000	0.0000	0.0000
	Total:	2.38e+001	3.54e+000	3.35e+000	22.3464	5.1110	5.9628
P	Mean:	7.08e+000	4.96e+000	2.12e+000	6.6405	7.3744	3.7756
	np x Std:	6.12e+000	3.67e+000	2.45e+000	0.3347	0.2655	0.1851
	Total:	1.32e+001	8.63e+000	4.57e+000	6.9752	7.6399	3.9607
Time-constant part of total error:							
	Mean:	1.85e+001	1.64e+001	1.74e+001	17.3214	24.4315	30.9771
	np x Std:	5.23e+001	3.76e+001	2.86e+001	43.2301	49.6953	44.9389
	Total:	7.08e+001	5.41e+001	4.61e+001	60.5514	74.1268	75.9161
Time-random part of total error:							
	Mean:	3.54e+001	1.29e+001	9.98e+000	33.2084	19.1793	17.7371
	np x Std:	6.65e+000	4.50e+000	3.57e+000	0.3952	0.3987	0.3942
	Total:	4.21e+001	1.74e+001	1.35e+001	33.6035	19.5780	18.1313
Total error per axis:							
	Mean:	5.39e+001	2.93e+001	2.74e+001	50.5297	43.6108	48.7142
	np x Std:	5.27e+001	3.79e+001	2.89e+001	49.4703	56.3892	51.2858
	Total:	1.07e+002	6.72e+001	5.63e+001	0.0000	0.0000	0.0000
Line of sight error:	87.7 [arcs]						

Table 8-2 presents the information of all signals (available from the output port tab of each block in the tree view of PEET) with signal numbering according to Figure 8-1.

Table 8-2: Signal data for scenario 1

Scenario: PointingSat (APE, ensemble)
Data: Signals (filtered, correlated)
Unit: individual SI
LoC: np = 3

3D Signal	Mean(x)	Mean(y)	Mean(z)	np*Std(x)	np*Std(y)	np*Std(z)
Sig. 1 (CRV):	7.27e-005	6.06e-005	6.54e-005	1.26e-004	1.05e-004	1.13e-004
Sig. 2 (CRV):	0.00e+000	0.00e+000	0.00e+000	2.18e-004	1.45e-004	7.27e-005
Sig. 4 (RP):	1.93e-005	1.35e-005	1.49e-005	0.00e+000	0.00e+000	0.00e+000
Sig. 5 (CRV):	1.00e-004	2.00e-004	8.00e-005	0.00e+000	0.00e+000	0.00e+000
Sig. 5 (RP):	1.26e-007	8.84e-007	7.75e-008	0.00e+000	0.00e+000	0.00e+000
Sig. 5 (D):	5.86e-008	8.50e-008	1.83e-008	0.00e+000	0.00e+000	0.00e+000
Sig. 6 (CRV):	1.00e-004	2.00e-004	8.00e-005	0.00e+000	0.00e+000	0.00e+000
Sig. 6 (RP):	1.93e-005	1.35e-005	1.49e-005	0.00e+000	0.00e+000	0.00e+000
Sig. 6 (D):	5.86e-008	8.50e-008	1.83e-008	0.00e+000	0.00e+000	0.00e+000
Sig. 7 (CRV):	1.94e-005	1.94e-005	1.70e-005	3.36e-005	3.36e-005	2.94e-005
Sig. 8 (RP):	1.76e-005	1.76e-005	1.17e-004	0.00e+000	0.00e+000	0.00e+000
Sig. 9 (RP):	1.75e-005	1.75e-005	1.24e-004	0.00e+000	0.00e+000	0.00e+000
Sig. 10 (CRV):	1.94e-005	1.94e-005	1.70e-005	3.36e-005	3.36e-005	2.94e-005
Sig. 10 (RP):	2.48e-005	2.48e-005	1.70e-004	0.00e+000	0.00e+000	0.00e+000
Sig. 12 (RP):	1.50e-001	1.50e-001	1.50e-001	0.00e+000	0.00e+000	0.00e+000
Sig. 13 (RP):	9.75e-007	9.75e-007	4.73e-007	0.00e+000	0.00e+000	0.00e+000
Sig. 14 (CRV):	1.94e-005	1.94e-005	1.70e-005	3.36e-005	3.36e-005	2.94e-005
Sig. 14 (RP):	2.48e-005	2.48e-005	1.70e-004	0.00e+000	0.00e+000	0.00e+000
Sig. 15 (CRV):	-1.70e-005	-1.94e-005	-1.94e-005	2.94e-005	3.36e-005	3.36e-005
Sig. 15 (RP):	1.70e-004	2.48e-005	2.48e-005	0.00e+000	0.00e+000	0.00e+000
Sig. 16 (CRV):	-1.70e-005	-1.94e-005	-1.94e-005	2.94e-005	3.36e-005	3.36e-005
Sig. 16 (RP):	1.25e-004	1.77e-005	1.72e-005	0.00e+000	0.00e+000	0.00e+000
Sig. 17 (CRV):	0.00e+000	0.00e+000	3.23e-023	0.00e+000	0.00e+000	5.59e-023
Sig. 17 (RP):	2.69e-006	3.40e-007	2.09e-007	0.00e+000	0.00e+000	0.00e+000
Sig. 18 (RP):	6.70e-008	6.70e-008	6.70e-008	0.00e+000	0.00e+000	0.00e+000
Sig. 20 (RP):	1.50e-001	1.50e-001	1.50e-001	0.00e+000	0.00e+000	0.00e+000
Sig. 21 (RP):	6.46e-007	8.42e-007	8.64e-007	0.00e+000	0.00e+000	0.00e+000
Sig. 22 (P):	3.43e-005	2.40e-005	1.03e-005	2.97e-005	1.78e-005	1.19e-005
Sig. 23 (RV):	2.18e-005	2.18e-005	2.18e-005	1.26e-005	1.26e-005	1.26e-005
Sig. 24 (RV):	2.18e-005	2.18e-005	2.18e-005	1.26e-005	1.26e-005	1.26e-005
Sig. 24 (P):	3.43e-005	2.40e-005	1.03e-005	2.97e-005	1.78e-005	1.19e-005
Sig. 25 (RV):	2.18e-005	2.18e-005	2.18e-005	1.26e-005	1.26e-005	1.26e-005
Sig. 25 (RP):	6.46e-007	8.42e-007	8.64e-007	0.00e+000	0.00e+000	0.00e+000
Sig. 25 (P):	3.43e-005	2.40e-005	1.03e-005	2.97e-005	1.78e-005	1.19e-005

3D Signal	Mean(x)	Mean(y)	Mean(z)	np*Std(x)	np*Std(y)	np*Std(z)
Sig. 26 (P):	2.40e-001	2.40e-001	9.90e-002	0.00e+000	0.00e+000	0.00e+000
Sig. 27 (P):	3.75e-008	3.75e-008	1.36e-008	0.00e+000	0.00e+000	0.00e+000
Sig. 28 (RV):	2.18e-005	2.18e-005	2.18e-005	1.26e-005	1.26e-005	1.26e-005
Sig. 28 (RP):	6.46e-007	8.42e-007	8.64e-007	0.00e+000	0.00e+000	0.00e+000
Sig. 28 (P):	3.43e-005	2.40e-005	1.03e-005	2.97e-005	1.78e-005	1.19e-005
Sig. 29 (CRV):	7.27e-005	6.06e-005	6.54e-005	2.52e-004	1.79e-004	1.35e-004
Sig. 30 (CRV):	1.68e-005	1.90e-005	1.90e-005	2.94e-005	3.36e-005	3.36e-005
Sig. 30 (RP):	1.16e-004	1.66e-005	1.62e-005	0.00e+000	0.00e+000	0.00e+000
Sig. 30 (D):	-1.01e-010	-1.56e-010	-8.05e-011	0.00e+000	0.00e+000	0.00e+000
Sig. 31 (CRV):	8.95e-005	7.96e-005	8.45e-005	2.54e-004	1.82e-004	1.39e-004
Sig. 31 (RP):	1.16e-004	1.66e-005	1.62e-005	0.00e+000	0.00e+000	0.00e+000
Sig. 31 (D):	-1.01e-010	-1.56e-010	-8.05e-011	0.00e+000	0.00e+000	0.00e+000
Sig. 32 (CRV):	8.95e-005	7.96e-005	8.45e-005	2.54e-004	1.82e-004	1.39e-004
Sig. 32 (RV):	2.18e-005	2.18e-005	2.18e-005	1.26e-005	1.26e-005	1.26e-005
Sig. 32 (RP):	1.16e-004	1.71e-005	1.63e-005	0.00e+000	0.00e+000	0.00e+000
Sig. 32 (P):	3.43e-005	2.40e-005	1.03e-005	2.97e-005	1.78e-005	1.19e-005
Sig. 32 (D):	-1.01e-010	-1.56e-010	-8.05e-011	0.00e+000	0.00e+000	0.00e+000

1D Signal	Mean	np*Std
Sig. 3 (RP):	4.96e-006	0.00e+000
Sig. 11 (RP):	1.50e-001	0.00e+000
Sig. 19 (RP):	1.50e-001	0.00e+000

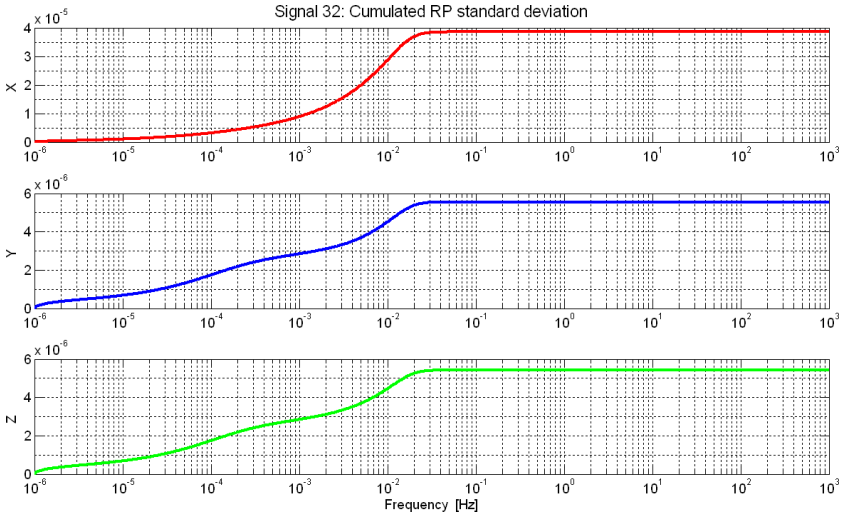

Figure 8-2: Cumulated standard deviation PEC RP signal

Figure 8-2 shows the cumulated standard deviation of the random process part of the input signal to the PEC block. It can be used to cross-check if all noise power in the signal is considered in the evaluation bandwidth. A flat level at the upper end reveals that

no significant noise power is added by higher frequency components of the signal and the evaluation bandwidth is chosen sufficiently large. In particular, for scenario 1, the bandwidth could even be decreased to about 0.1 Hz without significant change of the equivalent variance of the random process signal. This statement is however only valid for the random process part itself. In presence of significant periodic signals at high frequencies the evaluation bandwidth has to be maintained to keep them properly accounted for.

Result summary

According to Table 8-1 the final line-of-sight error for scenario 1 is 87.7 arcsec, thus the requirement of 90 arcsec (see chapter 4.3) is just met and almost no margin is present.

The time-constant and the time-random part contribute significantly to the total error: the driving time-constant part mainly via the equivalent standard deviation, the time-random part mainly via the equivalent mean.

The error around the line-of-sight axis (x) is significantly larger than the errors around the cross axes.

Among the time-random contributions to the x-axis error, those related to the random process signal part are dominant (followed by periodic and time-random variable parts with almost no contribution of the drift).

On the cross-axes, the time-random errors are mainly driven by the periodic and time-random variable signal parts followed by a smaller - but still significant - component of the random process part of the signal.

Using Table 8-2 together with Figure 8-1 or equivalently the tree view of PEET, the driving error contribution can be 'tracked back' to the pointing error sources[3]. In case of scenario 1 these are mainly the star tracker to telescope misalignments (constructive and launch effects, i.e. PES 1 and PES 2) for all three axis, while there is also a large contribution from the star tracker field-of-view and pixel noise (PES 6) on the x-axis which is however not relevant for the line-of-sight error in this case. Other contributors – although up to an order of magnitude smaller – are star-tracker thermal stability (PES 10) and thermo-elastic distortion (PES 9 and PES 10).

The most potential to 'physically' improve the pointing performance is thus to gain a better knowledge of the star-tracker to telescope misalignment (i.e. due to dedicated on-ground or in-flight calibration procedures). Alternatively, if a lower level of confidence (e.g. 2σ) could be allowed from a mission feasibility point of view, the pointing error margin could be significantly increased.

[3] Note that the ‚parallel' system approach described in chapter 6.3 would be a more suitable approach if the main interest is the identification of a single driving error source as it allows easy comparison of the individual source contribution in the tree-view by direct inspection of the input signals to the final summation block.

8.2.2 Scenario 2: RPE, temporal, 1σ (n_p = 1)

Table 8-3 summarizes the pointing error results available from the PEC block tabs in the tree view of PEET. As in the previous chapter the last three columns contain additional information about the reduction of the total error per axis in % assuming that the respective entry in the x,y,z-data columns of the same row would not be present .

Table 8-3: Pointing error for scenario 2 (NOTE: data unit is [arcsec])

```
Scenario:  PointingSat (RPE, temporal)
    Data:  Signals (filtered, correlated)
    Unit:  [arcs]
     LoC:  np = 1
```

		x	y	z	x(%)	y(%)	z(%)
Signal Contributions:							
CRV	Mean:	0.00e+000	0.00e+000	0.00e+000	0.0000	0.0000	0.0000
	np x Std:	0.00e+000	0.00e+000	0.00e+000	0.0000	0.0000	0.0000
	Total:	0.00e+000	0.00e+000	0.00e+000	0.0000	0.0000	0.0000
RV	Mean:	0.00e+000	0.00e+000	0.00e+000	0.0000	0.0000	0.0000
	np x Std:	2.00e+000	2.00e+000	2.00e+000	95.5695	99.3545	99.4534
	Total:	2.00e+000	2.00e+000	2.00e+000	95.5695	99.3545	99.4534
D	Mean:	0.00e+000	0.00e+000	0.00e+000	0.0000	0.0000	0.0000
	np x Std:	1.50e-010	2.32e-010	1.20e-010	0.0000	0.0000	0.0000
	Total:	1.50e-010	2.32e-010	1.20e-010	0.0000	0.0000	0.0000
RP	Mean:	0.00e+000	0.00e+000	0.00e+000	0.0000	0.0000	0.0000
	np x Std:	8.85e-002	1.12e-002	1.07e-002	0.0977	0.0016	0.0014
	Total:	8.85e-002	1.12e-002	1.07e-002	0.0977	0.0016	0.0014
P	Mean:	0.00e+000	0.00e+000	0.00e+000	0.0000	0.0000	0.0000
	np x Std:	6.50e-003	6.50e-003	2.23e-003	0.0005	0.0005	0.0001
	Total:	6.50e-003	6.50e-003	2.23e-003	0.0005	0.0005	0.0001
Time-constant part of total error:							
	Mean:	0.00e+000	0.00e+000	0.00e+000	0.0000	0.0000	0.0000
	np x Std:	0.00e+000	0.00e+000	0.00e+000	0.0000	0.0000	0.0000
	Total:	0.00e+000	0.00e+000	0.00e+000	0.0000	0.0000	0.0000
Time-random part of total error:							
	Mean:	0.00e+000	0.00e+000	0.00e+000	0.0000	0.0000	0.0000
	np x Std:	2.00e+000	2.00e+000	2.00e+000	100.0000	100.0000	100.0000
	Total:	2.00e+000	2.00e+000	2.00e+000	100.0000	100.0000	100.0000
Total error per axis:							
	Mean:	0.00e+000	0.00e+000	0.00e+000	0.0000	0.0000	0.0000
	np x Std:	2.00e+000	2.00e+000	2.00e+000	100.0000	100.0000	100.0000
	Total:	2.00e+000	2.00e+000	2.00e+000	100.0000	100.0000	100.0000
Line of sight error:		2.8 [arcs]					

Table 8-4 presents the information of all signals (available from the output port tab of each block in the tree view of PEET) with signal numbering according to Figure 8-1.

Table 8-4: Signal data for scenario 2

```
Scenario:  PointingSat (RPE, temporal)
    Data:  Signals (filtered, correlated)
    Unit:  individual SI
     LoC:  np = 1
```

3D Signal	Mean(x)	Mean(y)	Mean(z)	np*Std(x)	np*Std(y)	np*Std(z)
Sig. 1 (CRV):	0.00e+000	0.00e+000	0.00e+000	0.00e+000	0.00e+000	0.00e+000
Sig. 2 (CRV):	0.00e+000	0.00e+000	0.00e+000	0.00e+000	0.00e+000	0.00e+000
Sig. 4 (RP):	0.00e+000	0.00e+000	0.00e+000	3.16e-006	2.21e-006	2.44e-006
Sig. 5 (CRV):	0.00e+000	0.00e+000	0.00e+000	0.00e+000	0.00e+000	0.00e+000
Sig. 5 (RP):	0.00e+000	0.00e+000	0.00e+000	4.00e-008	2.94e-007	2.37e-008
Sig. 5 (D):	0.00e+000	0.00e+000	0.00e+000	4.23e-013	6.13e-013	1.32e-013
Sig. 6 (CRV):	0.00e+000	0.00e+000	0.00e+000	0.00e+000	0.00e+000	0.00e+000
Sig. 6 (RP):	0.00e+000	0.00e+000	0.00e+000	3.16e-006	2.23e-006	2.44e-006
Sig. 6 (D):	0.00e+000	0.00e+000	0.00e+000	4.23e-013	6.13e-013	1.32e-013
Sig. 7 (CRV):	0.00e+000	0.00e+000	0.00e+000	0.00e+000	0.00e+000	0.00e+000
Sig. 8 (RP):	0.00e+000	0.00e+000	0.00e+000	5.10e-006	5.10e-006	3.40e-005
Sig. 9 (RP):	0.00e+000	0.00e+000	0.00e+000	9.09e-008	9.09e-008	6.73e-007
Sig. 10 (CRV):	0.00e+000	0.00e+000	0.00e+000	0.00e+000	0.00e+000	0.00e+000
Sig. 10 (RP):	0.00e+000	0.00e+000	0.00e+000	5.10e-006	5.10e-006	3.40e-005
Sig. 12 (RP):	0.00e+000	0.00e+000	0.00e+000	2.54e-006	2.54e-006	2.54e-006
Sig. 13 (RP):	0.00e+000	0.00e+000	0.00e+000	1.65e-011	1.65e-011	8.01e-012
Sig. 14 (CRV):	0.00e+000	0.00e+000	0.00e+000	0.00e+000	0.00e+000	0.00e+000
Sig. 14 (RP):	0.00e+000	0.00e+000	0.00e+000	5.10e-006	5.10e-006	3.40e-005
Sig. 15 (CRV):	0.00e+000	0.00e+000	0.00e+000	0.00e+000	0.00e+000	0.00e+000
Sig. 15 (RP):	0.00e+000	0.00e+000	0.00e+000	3.40e-005	5.10e-006	5.10e-006
Sig. 16 (CRV):	0.00e+000	0.00e+000	0.00e+000	0.00e+000	0.00e+000	0.00e+000
Sig. 16 (RP):	0.00e+000	0.00e+000	0.00e+000	8.89e-007	1.26e-007	1.25e-007
Sig. 17 (CRV):	0.00e+000	0.00e+000	0.00e+000	0.00e+000	0.00e+000	0.00e+000
Sig. 17 (RP):	0.00e+000	0.00e+000	0.00e+000	2.20e-008	3.13e-009	1.87e-009
Sig. 18 (RP):	0.00e+000	0.00e+000	0.00e+000	9.10e-009	9.10e-009	9.10e-009
Sig. 20 (RP):	0.00e+000	0.00e+000	0.00e+000	1.27e-006	1.27e-006	1.27e-006
Sig. 21 (RP):	0.00e+000	0.00e+000	0.00e+000	5.48e-012	7.14e-012	7.33e-012
Sig. 22 (P):	0.00e+000	0.00e+000	0.00e+000	5.40e-010	3.60e-010	1.80e-010
Sig. 23 (RV):	0.00e+000	0.00e+000	0.00e+000	9.70e-006	9.70e-006	9.70e-006
Sig. 24 (RV):	0.00e+000	0.00e+000	0.00e+000	9.70e-006	9.70e-006	9.70e-006
Sig. 24 (P):	0.00e+000	0.00e+000	0.00e+000	5.40e-010	3.60e-010	1.80e-010
Sig. 25 (RV):	0.00e+000	0.00e+000	0.00e+000	9.70e-006	9.70e-006	9.70e-006
Sig. 25 (RP):	0.00e+000	0.00e+000	0.00e+000	5.48e-012	7.14e-012	7.33e-012
Sig. 25 (P):	0.00e+000	0.00e+000	0.00e+000	5.40e-010	3.60e-010	1.80e-010

3D Signal	Mean(x)	Mean(y)	Mean(z)	np*Std(x)	np*Std(y)	np*Std(z)
Sig. 26 (P):	0.00e+000	0.00e+000	0.00e+000	1.70e-001	1.70e-001	7.07e-002
Sig. 27 (P):	0.00e+000	0.00e+000	0.00e+000	3.15e-008	3.15e-008	1.08e-008
Sig. 28 (RV):	0.00e+000	0.00e+000	0.00e+000	9.70e-006	9.70e-006	9.70e-006
Sig. 28 (RP):	0.00e+000	0.00e+000	0.00e+000	5.48e-012	7.14e-012	7.33e-012
Sig. 28 (P):	0.00e+000	0.00e+000	0.00e+000	3.15e-008	3.15e-008	1.08e-008
Sig. 29 (CRV):	0.00e+000	0.00e+000	0.00e+000	0.00e+000	0.00e+000	0.00e+000
Sig. 30 (CRV):	0.00e+000	0.00e+000	0.00e+000	0.00e+000	0.00e+000	0.00e+000
Sig. 30 (RP):	0.00e+000	0.00e+000	0.00e+000	4.29e-007	5.41e-008	5.19e-008
Sig. 30 (D):	0.00e+000	0.00e+000	0.00e+000	7.27e-016	1.13e-015	5.81e-016
Sig. 31 (CRV):	0.00e+000	0.00e+000	0.00e+000	0.00e+000	0.00e+000	0.00e+000
Sig. 31 (RP):	0.00e+000	0.00e+000	0.00e+000	4.29e-007	5.41e-008	5.19e-008
Sig. 31 (D):	0.00e+000	0.00e+000	0.00e+000	7.27e-016	1.13e-015	5.81e-016
Sig. 32 (CRV):	0.00e+000	0.00e+000	0.00e+000	0.00e+000	0.00e+000	0.00e+000
Sig. 32 (RV):	0.00e+000	0.00e+000	0.00e+000	9.70e-006	9.70e-006	9.70e-006
Sig. 32 (RP):	0.00e+000	0.00e+000	0.00e+000	4.29e-007	5.41e-008	5.19e-008
Sig. 32 (P):	0.00e+000	0.00e+000	0.00e+000	3.15e-008	3.15e-008	1.08e-008
Sig. 32 (D):	0.00e+000	0.00e+000	0.00e+000	7.27e-016	1.13e-015	5.81e-016

1D Signal	Mean	np*Std
Sig. 3 (RP):	0.00e+000	8.12e-007
Sig. 11 (RP):	0.00e+000	6.41e-005
Sig. 19 (RP):	0.00e+000	6.41e-005

Figure 8-3 shows again the cumulated standard deviation of the random process part of the input signal to the PEC block. As for scenario 1, all relevant noise power is covered in the evaluation bandwidth which could be decreased to about 0.1 Hz without significant change of the equivalent variance of the random process signal if it is ensured that no periodic signals at higher frequencies are present (or at least that those are not driving).

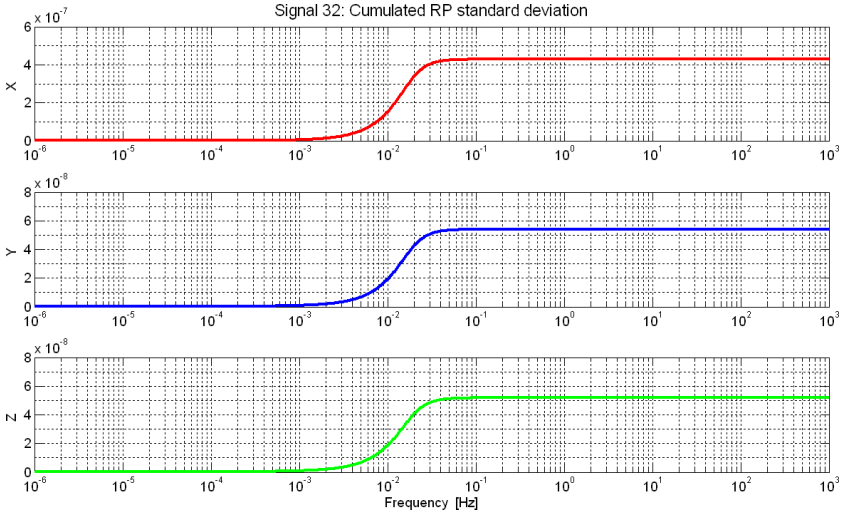

Figure 8-3: Cumulated standard deviation PEC RP signal

Result summary

According to Table 8-3 the final line-of-sight error for scenario 2 is 2.8 arcsec which violates the RPE requirement of 2 arcsec (see chapter 4.3).

The time-constant part of the error basically has no effect and the pointing error is purely defined by the standard deviation of the time-random contribution.

Among the time-random signal parts, only the time-random variable error is significant, random process, drift and periodic signals are negligible.

The error magnitude is identical for all individual axes, the larger line-of-sight error results from the combination of 2-axis information.

As only one RV type pointing error source is present in the PointingSat example, tracking the related pointing error source (random part of the thermo-elastic distortion, i.e. PES 10) is trivial. Consequently, to meet the requirement this single error source would have to be mitigated.

However - according to [AD1] - a random variable is only ‘suboptimal’ in a sense of system transfer modelling and application of metric filters as only worst-case approximations can be carried out. Thus, it might be beneficial to put effort in the modelling of the pointing error source itself, ideally to find an expression in terms of a random process which can be evaluated exactly (from a software and theoretical background point of view), even more when the error source is exceeding the pointing requirement as it is the case here.

8.2.3 Scenario 3: PRE, mixed, 3σ ($n_p = 3$)

Table 8-5 summarizes the pointing error results available from the PEC block tabs in the tree view of PEET. As for the APE scenario the last three columns contain additional information about the reduction of the total error per axis in % if the respective entry in the x,y,z-data columns is artificially set to zero .

Table 8-5: Pointing error for scenario 3 (NOTE: data unit is [arcsec])

```
Scenario:  PointingSat (PRE, mixed)
    Data:  Signals (filtered, correlated)
    Unit:  [arcs]
     LoC:  np = 3
```

		x	y	z	x(%)	y(%)	z(%)
Signal Contributions:							
CRV	Mean:	0.00e+000	0.00e+000	0.00e+000	0.0000	0.0000	0.0000
	np x Std:	0.00e+000	0.00e+000	0.00e+000	0.0000	0.0000	0.0000
	Total:	0.00e+000	0.00e+000	0.00e+000	0.0000	0.0000	0.0000
RV	Mean:	0.00e+000	0.00e+000	0.00e+000	0.0000	0.0000	0.0000
	np x Std:	0.00e+000	0.00e+000	0.00e+000	0.0000	0.0000	0.0000
	Total:	0.00e+000	0.00e+000	0.00e+000	0.0000	0.0000	0.0000
D	Mean:	0.00e+000	0.00e+000	0.00e+000	0.0000	0.0000	0.0000
	np x Std:	0.00e+000	0.00e+000	0.00e+000	0.0000	0.0000	0.0000
	Total:	0.00e+000	0.00e+000	0.00e+000	0.0000	0.0000	0.0000
RP	Mean:	0.00e+000	0.00e+000	0.00e+000	0.0000	0.0000	0.0000
	np x Std:	4.85e+001	6.37e+000	6.19e+000	99.4496	97.4822	98.2726
	Total:	4.85e+001	6.37e+000	6.19e+000	99.4496	97.4822	98.2726
P	Mean:	0.00e+000	0.00e+000	0.00e+000	0.0000	0.0000	0.0000
	np x Std:	2.67e-001	1.60e-001	1.07e-001	0.0015	0.0317	0.0149
	Total:	2.67e-001	1.60e-001	1.07e-001	0.0015	0.0317	0.0149
Time-constant part of total error:							
	Mean:	0.00e+000	0.00e+000	0.00e+000	0.0000	0.0000	0.0000
	np x Std:	0.00e+000	0.00e+000	0.00e+000	0.0000	0.0000	0.0000
	Total:	0.00e+000	0.00e+000	0.00e+000	0.0000	0.0000	0.0000
Time-random part of total error:							
	Mean:	0.00e+000	0.00e+000	0.00e+000	0.0000	0.0000	0.0000
	np x Std:	4.85e+001	6.37e+000	6.19e+000	100.0000	100.0000	100.0000
	Total:	4.85e+001	6.37e+000	6.19e+000	100.0000	100.0000	100.0000
Total error per axis:							
	Mean:	0.00e+000	0.00e+000	0.00e+000	0.0000	0.0000	0.0000
	np x Std:	4.85e+001	6.37e+000	6.19e+000	100.0000	100.0000	100.0000
	Total:	4.85e+001	6.37e+000	6.19e+000	100.0000	100.0000	100.0000

```
Line of sight error:      8.9 [arcs]
```

Table 8-6 presents the information of all signals (available from the output port tab of each block in the tree view of PEET) with signal numbering according to Figure 8-1.

Table 8-6: Signal data for scenario 3

Scenario: PointingSat (PRE, mixed)
Data: Signals (filtered, correlated)
Unit: individual SI
LoC: np = 3

3D Signal	Mean(x)	Mean(y)	Mean(z)	np*Std(x)	np*Std(y)	np*Std(z)
Sig. 1 (CRV):	0.00e+000	0.00e+000	0.00e+000	0.00e+000	0.00e+000	0.00e+000
Sig. 2 (CRV):	0.00e+000	0.00e+000	0.00e+000	0.00e+000	0.00e+000	0.00e+000
Sig. 4 (RP):	0.00e+000	0.00e+000	0.00e+000	2.46e-005	1.72e-005	1.90e-005
Sig. 5 (CRV):	0.00e+000	0.00e+000	0.00e+000	0.00e+000	0.00e+000	0.00e+000
Sig. 5 (RP):	0.00e+000	0.00e+000	0.00e+000	8.26e-008	1.62e-007	6.65e-008
Sig. 5 (D):	0.00e+000	0.00e+000	0.00e+000	0.00e+000	0.00e+000	0.00e+000
Sig. 6 (CRV):	0.00e+000	0.00e+000	0.00e+000	0.00e+000	0.00e+000	0.00e+000
Sig. 6 (RP):	0.00e+000	0.00e+000	0.00e+000	2.47e-005	1.72e-005	1.90e-005
Sig. 6 (D):	0.00e+000	0.00e+000	0.00e+000	0.00e+000	0.00e+000	0.00e+000
Sig. 7 (CRV):	0.00e+000	0.00e+000	0.00e+000	0.00e+000	0.00e+000	0.00e+000
Sig. 8 (RP):	0.00e+000	0.00e+000	0.00e+000	1.93e-005	1.93e-005	1.29e-004
Sig. 9 (RP):	0.00e+000	0.00e+000	0.00e+000	3.27e-005	3.27e-005	2.51e-004
Sig. 10 (CRV):	0.00e+000	0.00e+000	0.00e+000	0.00e+000	0.00e+000	0.00e+000
Sig. 10 (RP):	0.00e+000	0.00e+000	0.00e+000	3.80e-005	3.80e-005	2.82e-004
Sig. 12 (RP):	0.00e+000	0.00e+000	0.00e+000	1.68e-002	1.68e-002	1.68e-002
Sig. 13 (RP):	0.00e+000	0.00e+000	0.00e+000	1.09e-007	1.09e-007	5.30e-008
Sig. 14 (CRV):	0.00e+000	0.00e+000	0.00e+000	0.00e+000	0.00e+000	0.00e+000
Sig. 14 (RP):	0.00e+000	0.00e+000	0.00e+000	3.80e-005	3.80e-005	2.82e-004
Sig. 15 (CRV):	0.00e+000	0.00e+000	0.00e+000	0.00e+000	0.00e+000	0.00e+000
Sig. 15 (RP):	0.00e+000	0.00e+000	0.00e+000	2.82e-004	3.80e-005	3.80e-005
Sig. 16 (CRV):	0.00e+000	0.00e+000	0.00e+000	0.00e+000	0.00e+000	0.00e+000
Sig. 16 (RP):	0.00e+000	0.00e+000	0.00e+000	2.54e-004	3.31e-005	3.22e-005
Sig. 17 (CRV):	0.00e+000	0.00e+000	0.00e+000	0.00e+000	0.00e+000	0.00e+000
Sig. 17 (RP):	0.00e+000	0.00e+000	0.00e+000	5.45e-006	6.88e-007	4.26e-007
Sig. 18 (RP):	0.00e+000	0.00e+000	0.00e+000	1.24e-007	1.24e-007	1.24e-007
Sig. 20 (RP):	0.00e+000	0.00e+000	0.00e+000	1.26e-002	1.26e-002	1.26e-002
Sig. 21 (RP):	0.00e+000	0.00e+000	0.00e+000	5.44e-008	7.09e-008	7.28e-008
Sig. 22 (P):	0.00e+000	0.00e+000	0.00e+000	1.30e-006	7.77e-007	5.18e-007
Sig. 23 (RV):	0.00e+000	0.00e+000	0.00e+000	0.00e+000	0.00e+000	0.00e+000
Sig. 24 (RV):	0.00e+000	0.00e+000	0.00e+000	0.00e+000	0.00e+000	0.00e+000
Sig. 24 (P):	0.00e+000	0.00e+000	0.00e+000	1.30e-006	7.77e-007	5.18e-007
Sig. 25 (RV):	0.00e+000	0.00e+000	0.00e+000	0.00e+000	0.00e+000	0.00e+000
Sig. 25 (RP):	0.00e+000	0.00e+000	0.00e+000	5.44e-008	7.09e-008	7.28e-008
Sig. 25 (P):	0.00e+000	0.00e+000	0.00e+000	1.30e-006	7.77e-007	5.18e-007

3D Signal	Mean(x)	Mean(y)	Mean(z)	np*Std(x)	np*Std(y)	np*Std(z)
Sig. 26 (P):	0.00e+000	0.00e+000	0.00e+000	0.00e+000	0.00e+000	0.00e+000
Sig. 27 (P):	0.00e+000	0.00e+000	0.00e+000	0.00e+000	0.00e+000	0.00e+000
Sig. 28 (RV):	0.00e+000	0.00e+000	0.00e+000	0.00e+000	0.00e+000	0.00e+000
Sig. 28 (RP):	0.00e+000	0.00e+000	0.00e+000	5.44e-008	7.09e-008	7.28e-008
Sig. 28 (P):	0.00e+000	0.00e+000	0.00e+000	1.30e-006	7.77e-007	5.18e-007
Sig. 29 (CRV):	0.00e+000	0.00e+000	0.00e+000	0.00e+000	0.00e+000	0.00e+000
Sig. 30 (CRV):	0.00e+000	0.00e+000	0.00e+000	0.00e+000	0.00e+000	0.00e+000
Sig. 30 (RP):	0.00e+000	0.00e+000	0.00e+000	2.35e-004	3.09e-005	3.00e-005
Sig. 30 (D):	0.00e+000	0.00e+000	0.00e+000	0.00e+000	0.00e+000	0.00e+000
Sig. 31 (CRV):	0.00e+000	0.00e+000	0.00e+000	0.00e+000	0.00e+000	0.00e+000
Sig. 31 (RP):	0.00e+000	0.00e+000	0.00e+000	2.35e-004	3.09e-005	3.00e-005
Sig. 31 (D):	0.00e+000	0.00e+000	0.00e+000	0.00e+000	0.00e+000	0.00e+000
Sig. 32 (CRV):	0.00e+000	0.00e+000	0.00e+000	0.00e+000	0.00e+000	0.00e+000
Sig. 32 (RV):	0.00e+000	0.00e+000	0.00e+000	0.00e+000	0.00e+000	0.00e+000
Sig. 32 (RP):	0.00e+000	0.00e+000	0.00e+000	2.35e-004	3.09e-005	3.00e-005
Sig. 32 (P):	0.00e+000	0.00e+000	0.00e+000	1.30e-006	7.77e-007	5.18e-007
Sig. 32 (D):	0.00e+000	0.00e+000	0.00e+000	0.00e+000	0.00e+000	0.00e+000

1D Signal	Mean	np*Std
Sig. 3 (RP):	0.00e+000	6.33e-006
Sig. 11 (RP):	0.00e+000	1.88e-002
Sig. 19 (RP):	0.00e+000	1.88e-002

Figure 8-4 shows again the cumulated standard deviation of the random process part of the input signal to the PEC block.

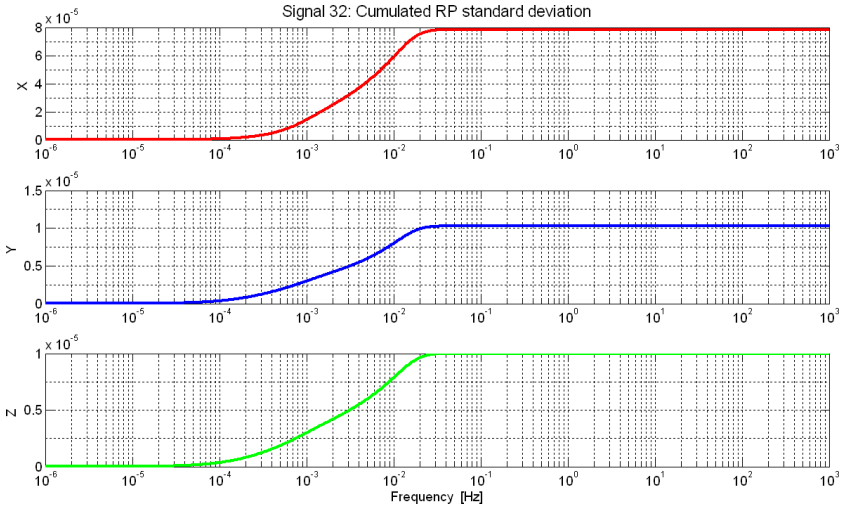

Figure 8-4: Cumulated standard deviation PEC RP signal

Also for this scenario all relevant noise power is covered in the evaluation bandwidth which could be decreased to about 0.05 Hz without significant change of the equivalent variance of the random process signal if it is ensured that no periodic signals at higher frequencies are present (or at least that those are not driving).

According to Table 8-5 the final line-of-sight error for scenario 3 is 8.9 arcsec, thus the requirement of 10 arcsec (see chapter 4.3) is met with 10% margin.

As for scenario 2 only the standard deviation of the time-random part contributes while the time-constant part has no effect. Furthermore, among the time-random contributions only the periodic signal part and the random process are present while the latter is about two orders of magnitude larger and can be considered as the only driver.

Although not contributing to the relevant line-of-sight error, the pointing error around the x-axis is approximately one order of magnitude larger than the cross-axis errors.

Using Table 8-6 together with Figure 8-1 (or equivalently the tree view of PEET), the driving error contribution can be ‘tracked back’ to the pointing error sources 5 and 6 which represent the star-tracker noise sources.

As the temporal noise (PES 5) contribution is exceeded by the field-of-view and pixel noise (PES 6) contribution by about one order of magnitude, improvement of the latter or selection of an alternative sensor with better specifications would be the key factor to mitigate the overall pointing error.

Analogous to the statement for scenario 1, application of a lower level of confidence for the error evaluation (if applicable/feasible) would provide more margin with respect to the requirement.

9 Remarks

It is important to note that above collection of PES is not intended to be exhaustive. Not in a sense that all possible error sources are covered and not in sense that all possible contributors to a single PES are set (e.g. PES 3 could comprise an additional thrust bias, PES 7 could have an additional ensemble distribution of the power spectrum, PES 10 could have a non-zero mean value, etc.).

The intention of the PES description is simply to cover all different kinds of error source representations.

The same is true for the realization of the system transfer models which should only show the basic predefined possibilities of PEET. Most of them are very simplified approximations of the real system behaviour only and not optimized to represent a ‘matching system’. However, in PEET it is up to the user define own system block types with arbitrary complexity of the models (by extending the existing PEET Matlab classes).